Data Centres as Prosumers: A Techno-Economic Analysis

UPPSALA UNIVERSITET

Master Thesis

Uppsala University

Jeremy Ericsson Sintong

Master of Science in Energy Technologies (MSc.ENTECH)

European Institute of Innovation & Technology (EIT) InnoEnergy

June 2023

Abstract

Rapid growth of digitalization has urged Data Centres (DC) to be more energy efficient by recovering waste heat from server racks that would otherwise be wasted. This techno-economic study is focused on upgrading low temperature waste heat from typical Air-Cooled DC for District Heating Network (DHN) market in Stockholm region. The methodology is carried out by four system configurations that are experimented with different historical electricity data, impacts of climate change with simulated weather data, and variations in DHN temperature as the heat supply scenario development. The results show that DC configuration with combination of both free-cooling and waste heat recovery can foster techno-economic benefits by reducing cooling consumption by 55.6%, compared to DC configuration with free-cooling only; and further lowering Power Usage Effectiveness (PUE) from 1.95 to 1.52. Lifecycle Operational Expenditure (LCO) has also been used as the economic indicator to represent the maximum initial investment that data centre should accept when deciding to recover the waste heat to the DHN. Moreover, the new technical Key Performance Indicators (KPIs) were introduced to support the decision-making in the supply of recovered waste heat to DHN. The electricity price was further identified to have greater impact than the effect of climate change for the overall techno-economic performance. On one specific hand, heat supply with Price-Limit scenario concluded that 40.18% of available waste heat from DC is not profitable should it be injected to DHN in the case of low electricity price. In the case when the electricity price is high, the amount of waste heat not injected to DHN increases to 58.57%.

Keywords

Data Centres, Prosumers, Techno-Economic Analysis, Waste Heat Recovery, District Heating, Heat Supply, Air-Cooled Data Centre

Acknowledgement

This thesis would have never been made without good support from people along its journey.

First of all, I'd like to express my sincere gratitude to my supervisor Nelson Sommerfeldt from KTH Royal Institute of Technology whose guidance and supervision have been so great to me. I also admire your patience to all my questions, with your constructive feedbacks and attention to details which have taught me a lot in doing this thesis. It's a true pleasure pursuing this thesis under your direct supervision.

This thesis also contributes to the research project "High Resolution GIS District Heating Source-Load Mapping" (project number 51538-1) funded by the Swedish Energy Agency's Termo program.

I'd like to extend my heartfelt gratitude to my subject reader Magnus Åberg from Uppsala University for his invaluable feedbacks and inputs in writing this thesis. Through some discussions that we've had, your suggestions were very useful in proceeding with the content of this thesis. Thanks for helping me to structure a good storyline through your advice and shared experiences. Your contributions to the work presented here have been great.

Besides, I'd like to thank my examiner Albert Mihranyan who's also the programme director of Master of Science in Energy Technologies (MSc. ENTECH) of European Institute of Innovation and Technology (EIT-InnoEnergy). Thanks for your guidance and leadership to the ENTECH programme.

All my friends and colleagues involved in ENTECH program and EIT-InnoEnergy, including Professors during my first year's master program in Instituto Superior Técnico in Lisbon, Portugal, also deserve my big thanks.

Special thanks are given to my all friends and communities whom I've been so grateful to spend my time with all of you along my master study journey. I will surely miss all sweet and hard moments in things that we did together.

Last and most importantly, I would never end up reaching this point without all support and everlasting love of my big family. Thanks for always being there for me through many ups and downs. Love you always.

Table of Contents

Abbreviations

AC	Air Conditioner
ASHRAE	American Society of Heating, Refrigerating, and Air-Conditioning Engineers
CAPEX	Capital Expenditures
COP	Coefficient of Performance
CPU	Central Processing Unit
CRAC	Computer Room Air Conditioner
CRAH	Computer Room Air Handling
CWR	Chilled Water Return
ERE	Energy Reuse Effectiveness
ERF	Energy Reuse Factor
EU	European Union
DASE	Direct Air Side Economizer
DC	Data Centre
DH	District Heating
DHN	District Heating Network
DHW	Domestic Hot Water
FC	Free Cooling
GHG	Greenhouse Gases
HP	Heat Pump
HSPF	Heating Seasonal Performance Factor
HT	High Temperature
IASE	Indirect Air-Side Economizer
IPCC	Intergovernmental Panel on Climate Change
IT	Information Technology
KPIs	Key Performance Indicators
LCO	Lifecycle Operational Expenditures
LT	Low Temperature
ODH	Open District Heating
OPEX	Operational Expenditures
ORC	Organic Rankine Cycle
O&M	Operation & Maintenance
PUE	Power Usage Effectiveness
SEK	Swedish Currency, Krona
SPF	Seasonal Performance Factor
WHR	Waste Heat Recovery

Nomenclatures

$COP_{HP,Carnot}$	Coefficient of Performance of Carnot Heat Pump
i	yearly timeframe
C_c	Cold side's fluid capacity rate
C_h	Hot side's fluid capacity rate
C_{max}	Maximum capacity rate
C_{min}	Minimum capacity rate
Cp_c	Cold side's fluid specific heat
Cp_h	Hot side's fluid specific heat
$\dot{E}_{DC,tot}$	Power Consumption in DC energy system (Total)
$\dot{E}_{aux.}$	Power Consumption of Auxiliary devices in DC energy system
$\dot{E}_{cooling,system}$	Power Consumption for Cooling Down the Server Racks
$\dot{E}_{IT}$	Power Consumption of operating IT Equipment
$H_{Discharge\_is}$	Enthalpy of Isentropic Discharge
H_{Evap_out}	Enthalpy of Evaporation Outlet
$H_{Suction}$	Enthalpy of Heat Pump Suction
H_S	Enthalpy of Heat Sink
$\dot{m}_c$	Cold side's fluid mass flow rate
$\dot{m}_h$	Hot side's fluid mass flow rate
$\dot{m}_{chiller}$	Mass Flow Rate of Chiller
$P_{Evap\_chiller}$	Evaporation Pressure of Chiller
$P_{cond.}$	Condensation Pressure
$P_{DC\_cooling}$	DC Cooling Power
$P_{HP,comp.}$	Power consumption to drive heat pump compressor
$\dot{Q}_{DH}$	Heat Output from Heat Pump (Heat Sink) injected to DHN
$\dot{Q}_{DC\_cooling}$	Thermal cooling energy of DC server racks
Q_L	Heat Input to Heat Pump (Heat Source)
$\dot{Q}_T$	Total heat transfer rate across heat exchanger
$\dot{Q}_{max}$	Maximum heat transfer rate across heat exchanger
r	Discount rate
$S_{Suction}$	Entropy of Heat Pump Suction
t	Hourly profile
T_{ci}	Cold side's inlet temperature
T_{co}	Cold side's outlet temperature
T_{hi}	Hot side's inlet temperature
T_{ho}	Hot side's outlet temperature
$T_{DC,Server(in)}$	Inlet temperature of hot-side heat exchanger that is the outlet temperature generated from server racks exhaust
$T_{DC,Server(out)}$	Outlet temperature of hot-side heat exchanger that is originally the server racks outlet temperature as the heat transfer medium

$T_{HSo,Evap(in)}$	Outlet temperature of cold-side heat exchanger that is the heat source inlet temperature of heat pump
$T_{HSo,Evap(out)}$	Inlet temperature of cold-side heat exchanger that is the heat source outlet temperature of heat pump
UA	Overall heat transfer coefficient of heat exchanger
W_{in}	Compression work (Net inlet work to Heat Pump)
ε	Effectiveness of Heat Exchanger
η_{comp}	Isentropic efficiency of compressor
$\eta_{supp,DH.}$	Efficiency of supplying heat to District Heating

Units

˚C	Degree Celsius
GJ	Giga Joule
GW	Gigawatt
GWh	Gigawatt hours
h	Hours
J	Joule
K	Kelvin
kg	Kilogram
kJ	Kilo Joule
kW	Kilowatt
kWh	Kilowatt Hours
L	Litre
MJ	Mega Joule
MW	Megawatt
MWh	Megawatt Hours
m	meter
m^2	Square meters
m^3	Cubic meters
s	Second
W	Watt

List of Figures

List of Tables

1. Introduction

Human activities have caused global warming which is likely to reach 1.5ºC between 2030 and 2052, if it continues to increase at the current rate [1]. Heating and cooling which currently represent around 50% of the EU's final energy consumption are among substantial sectors to conduct energy efficiency effort where global warming has been worsened by continuous emissions [2]. In 2021, production through district heat has increased by around 3% compared to 2020 and has met nearly 8% of final heating demand globally in buildings and industry [3]. Capturing waste heat in urban areas is one of effective methods to improve energy efficiency and reduce greenhouse gas emissions in cities. Market availabilities and technical supports on policies framework for such excess heat utilization are mostly dominant in Northern European hemisphere. There are already existing collaborations between heat provider companies and industrial partners that provide excess heat in Sweden [4]. Stockholm Exergi's Open District Heating (ODH) enables large waste heat prosumers to sell excess heat from their facilities into the ODH network [5]. Data Centres (DCs) have already been identified as potentially the greatest carbon-free heat sources for the Stockholm region's district heating network, accounting for 45.4% of total potential share of heat sources [6]. As of 2022, there are 92 data centres in Sweden according to the data from CloudScene [7]. Global data centre electricity usage in 2021 stood at 220-320 TWh, or approximately 0.9-1.3% of global final electricity demand, but this excludes energy used for cryptocurrency mining, which was 100-140 TWh in 2021 [8]. Such rapid growth of digitization has urged data centres facilities to become more agile and efficient, in terms of becoming not only consumers but also producers. Data Centre as energy prosumers considers part of their energy needs from their owned data processing facilities while using available distribution network to inject excess production from their existing facilities in the form of waste heat.

1.1 Knowledge Gap and Objectives

Predominantly, research studies on data centres waste heat recovery have provided thorough understanding and acquired critical importance to harness the potential use of such excess heat from data centres. Ebrahimi K. et al. [13] conducted a literature survey regarding some technologies of waste heat recovery (WHR) from DCs excess heat and concluded that absorption cooling and Organic Rankine Cycle (ORC) were identified to be among the most promising technologies for DCs waste heat reuse. However, their application depends solely on the quality of the recovered heat according to thermodynamic conditions and it still lacks clear determinations of associated

parameters to correlate the waste heat upgrade with specific economic and market phenomena.

In such regard, some studies have proven viabilities of instead utilizing DC's waste heat for district heating (DH) application. It obtained real-life applications within different regions and associated impacts as well. For instance, M. Wahlroos et al. [23] analysed the overall system efficiency of DC's waste heat utilization in Finland from the perspectives of both DC owners and DHN operators as one system. By having high shares of waste heat in DHN system (i.e., 20-60 MW), the system operational cost saving could be reached up to 7.3% in their case study. J. Yu et al. [25] simulated a novel heat recovery from DC in Harbin, China, to shift between space cooling and heating for secondary buildings such as apartment, offices, and fitness centres. The result indicated that the proposed system had better operational costs, being 458.3 thousand yuan lower than the one with air source heat pump system only. G.F. Davies et al. [35] investigated DCs waste heat reuse in London and they found that a WHR system in 3.5 MW data centre could lead to savings of over 4000 tons of CO_2 eq., and nearly £1 million per year by using heat pump for DH application.

To analyse the impact of DC's waste heat utilization, technical metrics must be incorporated for measuring the energy performance in DC itself. Generic DC energy efficiency metric such as Power Usage Effectiveness (PUE) is widely used and can be defined as total annual energy divided by total annual energy used for the IT power [39]. However, PUE associated variables are difficult to measure when facilities or primary equipment are shared [40]. PUE shouldn't be used alone as the only technical metric since the value of the reused energy with waste heat utilization is not considered. Another proposed metric for a typical DC to include waste heat recovery is the energy reuse effectiveness (ERE) as proposed by Zimmermann et al. [41]. However, the disadvantage of this ERE is that no difference is accommodated between energy forms in terms of their quality. While the energy input of the DC is electric energy, reuse energy extracted from the system is thermal energy, creating different exergy levels. On one specific hand, E. Oró et al. [24] studied energetic and economic feasibility of different WHR solutions in Air-Cooled DC and came up with conclusion that energy reuse factor (ERF), which can be defined as reused energy divided by total power consumed by DC, resulted the best metric to quantify WHR integration. The study concluded positive outcome from technical standpoint but negative output in economic. For instance, the metric indicated that the primary energy reused can be above 50%, but the economic result performed for a specific 1000 kW data centre located in Barcelona (Spain) demonstrated the non-viability of heat recovery integration in most of the conventional air-cooled data centres. This thesis project hereby intends to utilize multiple Key Performance Indicators (KPIs) to

correlate both technical and economic performance metrics for supporting the decision making whether waste heat recovery system from DC is techno-economically feasible or not, being applied specifically to Stockholm region, in Sweden.

All related research studies to the author's best knowledge have in common that they were conducted with assumption of fixed price of electricity price, which could be one of the most important parameters for DC's performance in supplying their waste heat to DHN. The fact electricity varies from year to year makes it important to be part of the analysis, to see how it affects the operational costs measured by the profitability of operating heat pump. Furthermore, the effect of climate change that contributes to changing outdoor temperature is also deemed non-trivial, due to the fact different outdoor temperature distributed throughout the year will also affect DHN conditions, both in price and network temperatures. It will also lead into heat supply profitability in terms of how much recovered heat can be sold to the DHN, noting the variety of outdoor temperature. This thesis project is intended to help compliment all mentioned studies by also utilizing newly proposed KPIs that can be applied for real-life market situation. The multiple results of different system configurations defined in the methodology part are then compared to obtain conclusions which shall be able to answer research questions and help support in making decisions, for DC owners to consider their roles in DHN market.

The overall aim of this thesis is to provide techno-economic analysis for DC's owners to consider recovering their waste heat to DHN. The primary objective is to identify both technically and economically viable heat recovery available from data centres in the ODH Market in the Stockholm region. Profitability of data centre waste heat is investigated with applicable heat pricing structures as utilizing waste heat for ODH Network will require additional electricity to drive a heat pump. Different system configurations are proposed, capable of using computational demands and air temperature as an analytical input, with electricity demand and waste heat as the output. The techno-economic analysis is performed with hourly prices from the NordPool Spot Electricity and ODH markets, to derive a management strategy that maximizes economic benefits, resulting in a final heating supply profile from data centre.

The subgoal of the thesis is to obtain in-depth insights of implementing the overall objective. Specifically focused on Air-Cooled DC's cooling technology, different system configurations are built to generate DC's recoverable heat which is upgraded by the heat pump. The complex relationship between electricity prices and feed-in heat prices is included, making it non-trivial to assess the economically recoverable heat. It intends to give clear understanding to DC owners pertaining to some benefits that can be offered upon upgrading waste heat from DC for DHN. Different system configurations correlated

with applicable market phenomena will enrich the perspectives of the techno-economic assessment, contributing to higher efficiency in urban heating systems. The main outcome is also expected to measure potential benefits of upgrading the original low-quality of heat of data centres.

1.2 Research Questions

Some research questions are included hereby as part of work scope and defined boundaries, on which the thesis is geared towards certain directions.

1. In which system configuration will the DC energy system produce the most favourable performance?
2. What techno-economic benefits will the configuration(s) have when compared to stand-alone DC without WHR?
3. How do outdoor temperature and electricity price influence the performance of each system configuration?

The satisfaction of research questions from the model will be demonstrated in the conclusion part of the thesis, which also includes techno-economic assessment that suits the ODH network conditions. Whether the upgraded heat from DCs waste heat can satisfy the full demand of open district heating network is not the scope of the project, as the thesis aims are originated from the perspective of DCs owners who are considering new investment in WHR, and that can take active contributions in increasing the efficiency of district heating systems.

2. Background

Excess heat from DCs is determined mainly from the cooling processes for Information Technology (IT) equipment in server halls. Heat is produced in several server components, especially processors, memory chips, and disk drives [9]. By supplying excess heat from data centre to District Heating Network (DHN), DC owners can reduce their direct operational costs by re-converting the waste heat produced from their cooling system, while the DHN Operator obtains heat to increase the heat capacity in the network, avoiding such needs to invest in centralized-baseload heat production capacity.

2.1 Overview of Data Centres Energy Systems

Data Centre is an energy intensive facility which large power at typically constant rate. This large power consumption is mainly due to IT equipment which includes Central Processing Unit (CPU), cooling loads, lighting, building switchgear and protection device, power conditioning as well as network equipment. The IT equipment and cooling load demand are two largest contributors to a typical data centre facility as depicted in the figure 1.

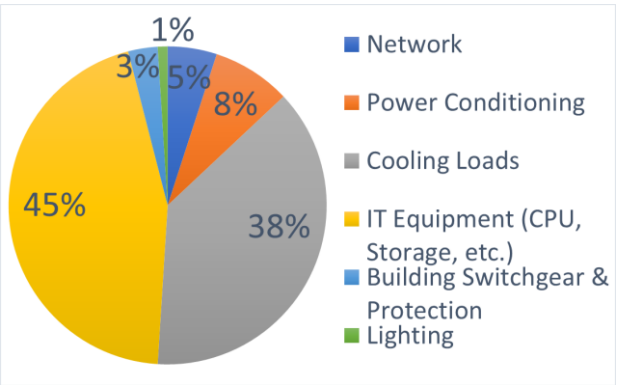

Figure 1. Power Consumption Distribution in Data Centre [adapted from 10]

During normal operation, IT equipment such as server racks must be cooled, whilst the requirement for cooling system must adhere specific temperatures and air quality standard. ASHRAE Thermal Guidelines represent the temperature and humidity requirement, should the IT equipment meet the stable and reliable operations in data processing facilities. For all suitable classes, the recommended dry bulb temperature for cooling supply is within 18–27ºC while the humidity range is desired to be between 50–70% which is spanned from minimum -9ºC to maximum 15ºC from the Dew Point [11].

Because of large variances in DCs heat dissipation rates, various cooling techniques have been developed to satisfy such different cooling needs. For instance, the conventional DCs has heat dissipation rates in the range of 430–861 W/m². With more compact high power modules development in the newer DCs generations, the heat dissipation rates have increased at least 10 times to 6,458–10,764 W/m², which describes the power consumption of IT equipment (W) divided by the area occupied by all IT rack enclosures (m²) [12].

2.2 Data Centre Cooling System

There are three cooling technologies being used in the data centres nowadays. Those are air-cooled, water-cooled, and two-phase cooled cooling systems [13]. Most of the existing data centres adopt air-cooled technology which produce low-grade waste heat from the cooling system [15]. The different cooling approaches are varied in accordance to working fluid used, heat dissipation rate from specific types, sizes of server racks, and associated temperatures in the overall cooling process or systems. In this thesis work, the focus will be dedicated for waste heat upgrade from air-cooled system.

In typical DCs legacy, server racks are comparted into cold and hot aisle. Typical configurations of air-cooled system in respect to their cooling provider is divided into four types, namely Computer Room Air Conditioner (CRAC) and Computer Room Air Handler Units (CRAH), in-row cooling, and rear-door cooling [15]. What distinguishes one configuration to another is practically related to the size of DCs applied. CRAC is normally used in small DCs (<100 kW) while CRAH is compatible with medium-big size DCs (>100 kW). In-row cooling and rear-door cooling system can be utilized for medium to high application (> 10 kW per rack) and high application (> 35 kW). From the perspective of cold air utilized, there's a difference between CRAC and CRAH as well [24]. CRAH uses cold air that's cooled through water which is cooled outside the data centre using a cooling chiller. On the other hand, CRAC utilizes cold air that's cooled directly by a coolant which is then cooled in the outside condenser. The difference between CRAH and CRAC schematics can be seen in the following figure 2 and 3.

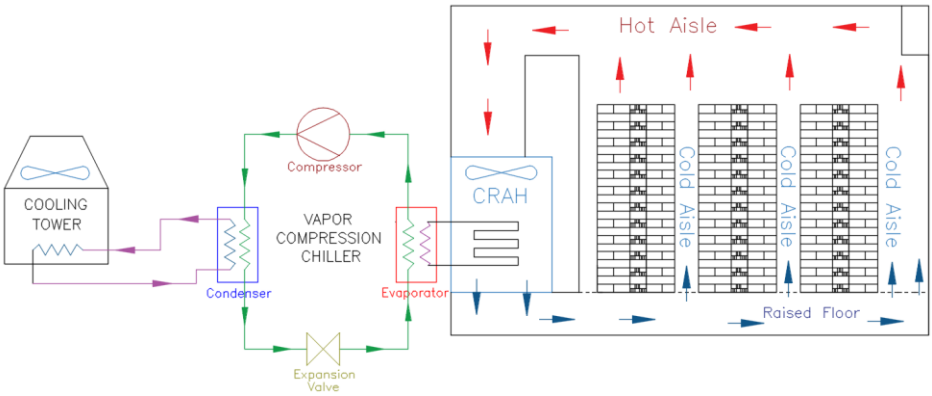

Figure 2. CRAH Schematic Diagram in Data Centre Air-Cooled System [adapted from 24]

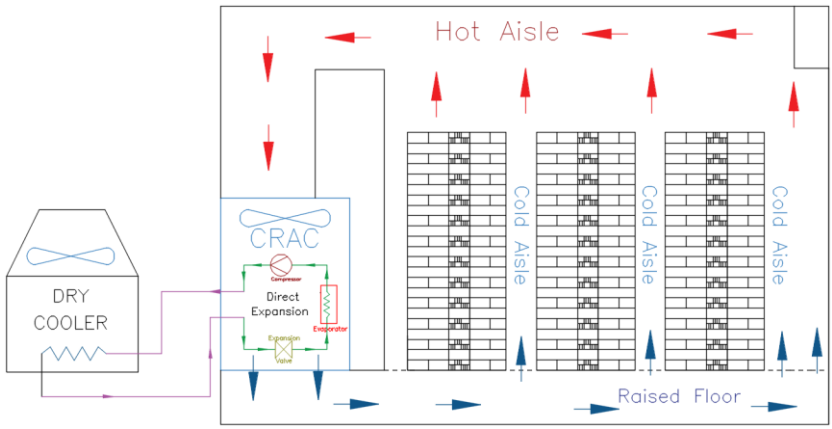

Figure 3. CRAC Schematic Diagram in Data Centre Air-Cooled System [adapted from 24]

Cold aisle provides cool intake air to each server racks, which can go either through floor pendulums or ceiling diffuser. On opposite sides, hot aisle dissipates heat from such server cabinets and return it back to the intake of cooling system. Heat dissipation of hot air returning from the server racks is rejected to outdoor atmosphere by utilizing a chiller and cooling tower loop.

There is also a cooling technology that takes advantage of available free air from outdoor, so-called free cooling system. Free cooling technology can be implemented in the air-cooled system by using a mixture of outdoor air and a recirculation system through automatic air mixing system [31]. The system uses different economizer configurations to meet the cooling criteria of DCs. There are two types of free air-cooling systems in typical DCs, namely Direct Air-Side Economizer (DASE) and Indirect Air-Side Economizer (IASEs) [32].

DASE is categorized as direct evaporative cooling system since the ambient air traverses the media, reducing dry bulb temperature, while being delivered to the space. On the other hand, IASEs is technically an Air-To-Air Heat Exchangers systems due to the fact ambient air is utilized to indirectly cool the recirculating airstream without delivering ambient air to the space. Free cooling system pertains to taking advantages of low outdoor temperature to be utilized for DCs cooling demand.

2.3 Waste Heat Recovery from Data Centres

Low waste heat temperature from DC can be boosted using heat pumps [35]. Depending on the working conditions of DC server racks, the return air temperature can reach as high as 47 ºC [24]. This low-grade quality of waste heat requires heat pump to meet 68 ºC of DHN temperature minimum requirement in Stockholm's ODH market [5]. Waste heat upgrade for DHN purpose requires waste heat recovery technique that enables efficient heat exchange from the main source of DC waste to the desired temperature. It's also important to choose the specific locations of boosting temperatures from data centres waste heat. For the air-cooled system, one of the optimum locations to capture heat in air-cooled DCs facilities for maximum energy capture is at the rack exhaust prior to room air mixing [15]. WHR in the exhaust occurs in the common duct before the air handling units [47]. Figure 4 demonstrates the schematic diagram of the location of waste heat recovery technique used from typical Air-Cooled DC system.

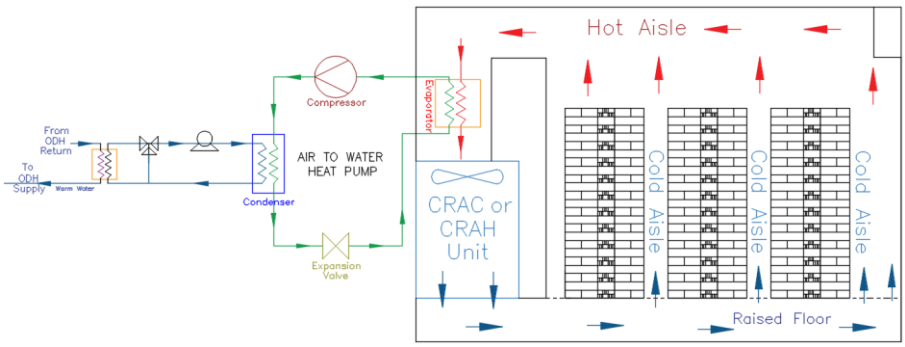

Figure 4. Schematic of waste heat recovery technique at the airside (hot aisle) for Air-Cooled System [adapted from 15]

2.4 Heat Pump

Heat pump has gained its momentum nowadays. The world's energy demand keeps growing, while the increasing fossil-based energy use has caused an energy crisis [17]. A heat pump possesses all main parts in a package unit, described in other words as reverse direction of typical refrigeration machine.

The main components of compression heat pump cycle are compressor, expansion valve, condenser, and evaporator [19]. Apart from the main components, heat pump also has some other working package which consists of piping works, heat source, heat sink, and control system. Heat pump is an energy technology device which incorporates thermodynamic principles to upgrade the heat from heat source to higher degree in heat sink.

The working fluid inside the heat pump is called refrigerant, which is crucial to generate heating effect in the heat sink due to its low boiling point. In terms of heat sources utilized, heat pump can be categorized into two types, namely primary heat pump and secondary heat pump [18]. Primary heat pump utilizes natural substances as heat sources such as air, soil, and ground/surface water. On the other hand, secondary heat pump reuse waste heat as heat source, which may come from extracted air, wastewater, and waste heat from rooms to be cooled. In respect to data centres as producer of energy, the secondary heat pump is applied to increase the thermal energy from waste heat of data centre cooling and satisfy district heating requirement.

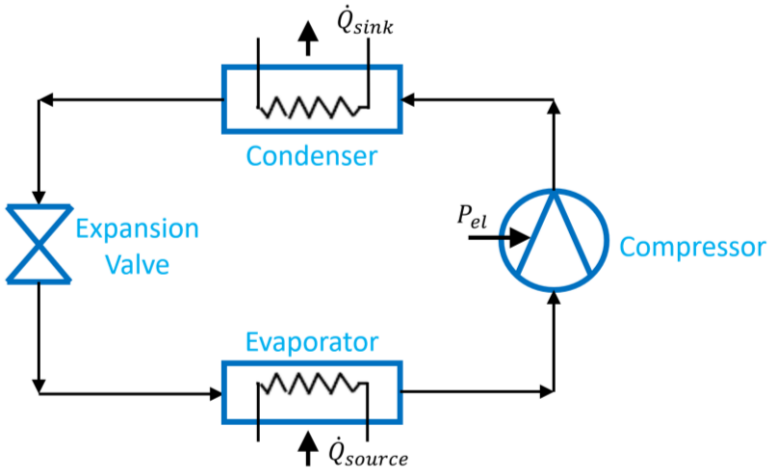

Figure 5. Basic flow chart of vapor compression cycle

Figure 5 demonstrates basic flow chart of heat pump cycle with vapor compression system which consists of four main parts: namely expansion valve, evaporator, compressor, and condenser. Heat source (or $\dot{Q}_{source}$) is used to evaporate the refrigerant while heat sink (or $\dot{Q}_{sink}$) extracts the heat from the boiled refrigerant. The refrigerant mixture gets evaporated in the evaporator, resulting in the superheat to a few degrees. A separator is in most case needed to prevent liquid from entering the compressor. The heat pump is operated with electricity to run the compressor (P_{el}) to increase refrigerant pressure before entering the condenser, maintaining the proper thermal condition for heat transfer process from the refrigerant to the heat sink. In the condenser,

the superheated vapor coming from the compressor is de-superheated, then condensed into liquid form with some degree of sub-cooling, to prevent the vapor entering the expansion valve. The expansion valve brings the refrigerant from the condenser pressure to the one of the evaporators. When the cold refrigerant flows through the evaporator, the refrigerant absorbs the heat from the heat source in the evaporator and gets boiled. The heat pump cycle runs continuously to produce the desired heat.

Unlike conventional combustion processes that acquire fossil fuel as primary energy, heat pumps can be energized from clean renewable electricity. While combustion processes cost energy loss at the end products (i.e., efficiency is less than 1), heat pump efficiency is measured with Coefficient of Performance (COP) in such degree where the value is always more than 1. The determination of COP from heat pump cycle is adhered to the following equations 1 and 2.

$$COP = \frac{\dot{Q}_{sink}}{P_{el}} \quad \text{(Eq. 1)}$$

$$COP = Eff_c \cdot \frac{T_c}{T_c - T_e} \quad \text{(Eq. 2)}$$

COP characteristic of compression heat pump can also be determined using Carnot Efficiency (Eff_c) principle, dividing condensing temperature (T_c) with the difference between Tc and evaporator temperature (T_e), and then multiplied by Eff_c value [21].

2.5 District Heating and Open District Heating Network

DH is a network of heat distribution that transports heat in the forms of hot water to end-customers through thermal substations. DHN encompasses two main distribution pipes, so called DHN Supply and DHN Return line. The DHN supply line contains the main hot fluid that delivers thermal service in the form of hot water to the end-customers, while the return line is the output effect from customer substations that's recirculated back to the DHN main processing plant.

ODH network is a marketplace for district heating in the city where any companies with suitable amount of excess heat in their facilities can take active roles to supply energy in the forms of warm water to local adjacent of available district network connection nearby. Main concern is regarding the quality of such amounted excess heat that can be channelled to the available ODH flow line. The related company or business is required to boost the temperature of their excess heat for instance, when the excess heat from any of their facilities is below the minimum requirement to meet thermal grade standard of the ODH

network. Stockholm Exergi is the operator of the ODH network in Stockholm, Sweden. The focus of DC as producer of energy is imposed to energy generation in the forms of thermal heat and that take roles as the heat supplier in the ODH business model with Stockholm Exergi. Specific focus is geared towards ODH Call contract model only. This type of model is the best fit for heat suppliers which have good stability levels of heat generation profile throughout the day and year [5].

In ODH Call model, the agreement of levels of capacity is confirmed by both Stockholm Exergi and heat suppliers before supplying the heat to the ODH network. In this scheme, Stockholm Exergi will make a request for the heat with a guarantee to the heat supplier that the request is always present as long as the outdoor temperature is 12˚C or below [5]. The temperature supplied to the ODH flow line is typically 68˚C but can be also higher in certain cases. ODH Call can be also described as on-demand heating and its compensation level also differs. For instance, the lower the outdoor temperature, the higher the heating demand for end-use thermal service. The contract model between Stockholm Exergi and excess heat supplier is long term [4]. The contract for ODH Call is typically signed for 10 years with the right for the excess heat supplier to extend the contract for another 5 years, while the compensation level in the contract is indexed annually [4].

3. Methodology

To answer the research questions, there are experiments to be done by initially setting up system configuration which will tell us the techno-economic performance of data centre. Four different system configurations are experimented with each modelling scope and formulations through defined equations. Each model is scoped by applicable boundary conditions which consist of server rack operation, cooling system, free cooling system, waste heat capture, and waste heat upgrade. Each typical model from one configuration to another is used as applicable.

Different tasks are then assigned to each system configuration in accordance with historical electricity data, impacts of climate change with simulated weather data, and variations in DHN temperature as heat supply scenario development. The detailed computational demand of each configuration is then examined with Key Performance Indicators (KPIs), both in terms of technical and economic KPIs. The techno-economic performance of each configuration is explained in each related sub-chapter.

3.1 System Configurations

Both waste heat recovery (WHR) and free cooling (FC) option are the main differentiators in each configuration, having either one of them or both to be included in the system. The location to perform WHR is done at the highest possible waste heat temperature location, that is in the hot aisle compartment. FC option is considered in this thesis work, mainly driven by cold climate condition in Stockholm because low outdoor air temperature can be harnessed by doing such FC option. The FC location is performed adjacent to the DC's existing cooling system to ensure that the cooling air supply temperature to server racks is always guaranteed as the outdoor temperature is not always all the time satisfied, especially during summer. Each given configurations intends to motivate whether WHR and/or FC will provide benefit(s) compared to DC's operational baseline, or in other words a DC being operated as business-as-usual (BaU). The overall impacts will be demonstrated in Key Performance Indicators (KPIs) part.

3.1.1 System Configuration A1: DC without WHR & without FC

The first system configuration is established as a baseline of DC operation where a conventional cooling system is used to cool down server racks. It represents BaU scenario in which DC's server racks are cooled but the waste heat is not recovered. The cooling system in this configuration isn't equipped with free cooling option. A schematic diagram of system configuration A1 can be seen on the following figure 6.

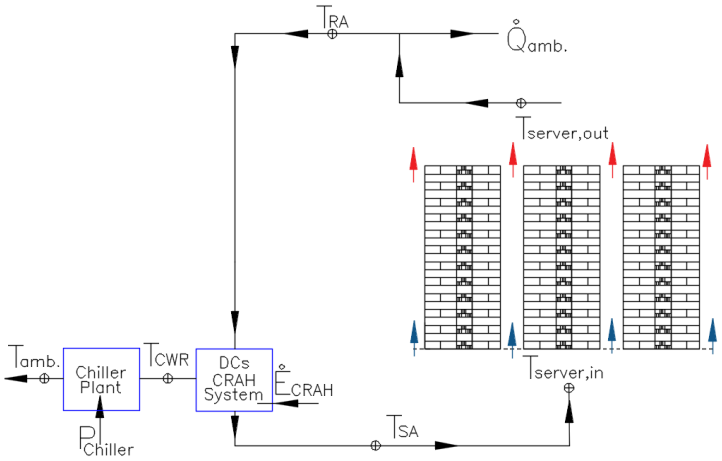

Figure 6. System Configuration A1

The exhaust air coming out from the server racks located in the hot aisle is called return air (RA). This RA is brought back to the CRAH system before being utilized again as supply air (T_{SA}) to cool down the server racks. Return air temperature (T_{RA}) depends on server utilization and thus its values vary accordingly with hourly server operation.

3.1.2 System Configuration A2: DC without WHR & with FC

In this configuration, FC is added to the data centre cooling system from configuration A1. Indirect Air-Side Economizer is chosen for this FC model as developed by Park, S. [38]. This type of FC model is chosen due to its ability to avoid condensation problems by not directly supplying outdoor air to server racks. System configuration A2 can be depicted in figure 7.

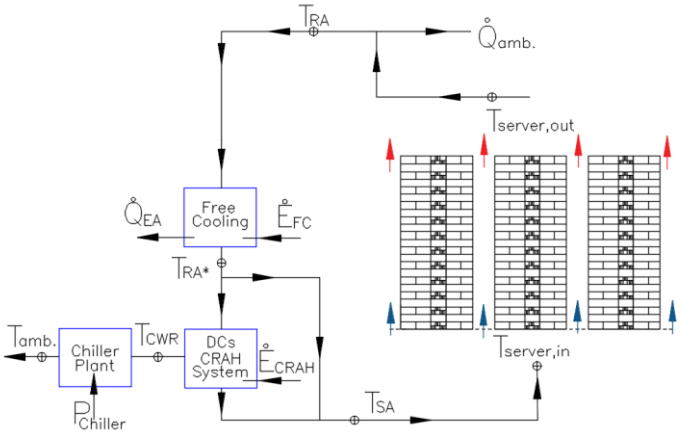

Figure 7. System Configuration A2

Return air temperature (T_{RA}) represents the exhaust heat from DC server racks as the input parameter for FC model. Secondary return air temperature (T_{RA*}) is output from free cooling model and passes through the primary indirect-heat exchanger.

3.1.3 System Configuration A3: DC with WHR & without FC

This third configuration demonstrates a development of configuration A1 by upgrading the waste heat generated without including free cooling system. The overall sequential configuration is started from waste heat generation from DC cooling system, followed by harnessing the waste heat with heat exchange process, and then the heat pump is used to boost the waste heat temperature before being injected to DHN. A heat pump is operated according to the generated waste heat profile and the supply temperature of DHN. System configuration A3 can be seen in figure 8.

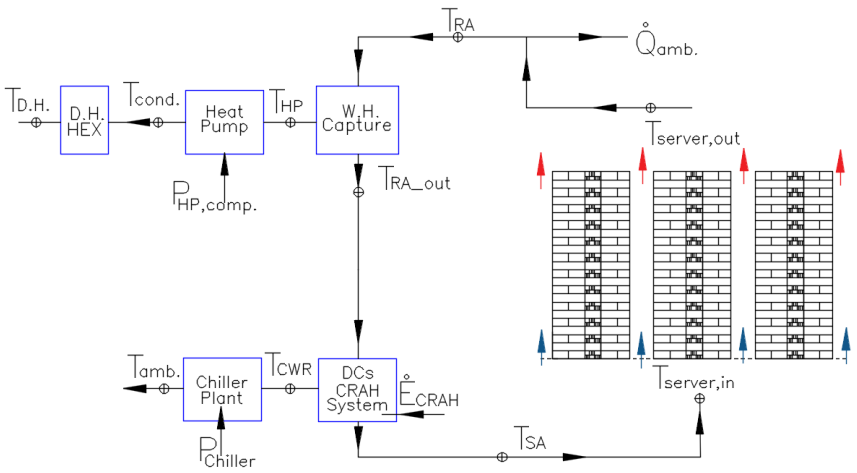

Figure 8. System Configuration A3

3.1.4 System Configuration A4: DC with both WHR & FC

System configuration A4 is compiled as a fully integrated model to include both FC in DC cooling and a WHR system. The model from the previous three configurations is combined in this last configuration. DC server rack operation and DC cooling model are taken from the first configuration, while adapting FC and WHR model from the second and third configuration respectively. Figure 9 shows the schematic of system configuration A4.

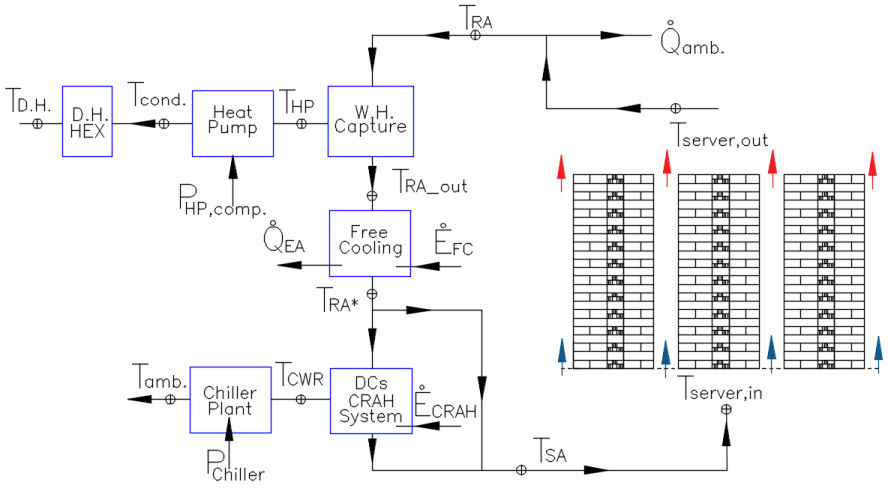

Figure 9. System Configuration A4

3.2 Modelling Scope and Formulations

An integrated approach for each system configuration is divided into three sub-models, namely server rack operation, DC cooling system, and waste heat recovery (WHR) system which can be segmented according to figure 10.

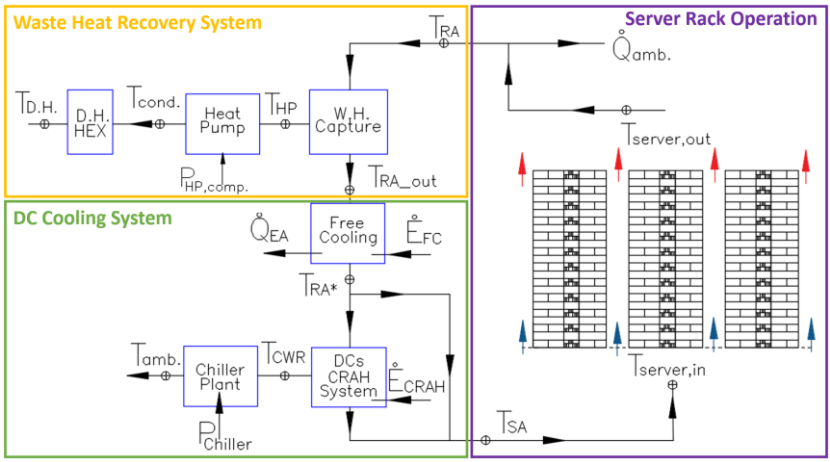

Figure 10. Modelling Approach for Each System Configuration

The server rack operation model produces a waste heat profile from DC server racks. WHR system is divided into two parts, waste heat capture and waste heat upgrade. DC cooling system also includes free cooling.

3.2.1 Server Rack Operation

The server rack operation model is adapted from the simplified server model proposed by Ham S.W. et al. [27]. The model describes general overview to simplify the DCs internal server heat generation that has high degree of fluctuation, depending on how DCs process their data input. The model is examined with server racks operational conditions to generate hourly profile of exhaust temperature of DC server racks.

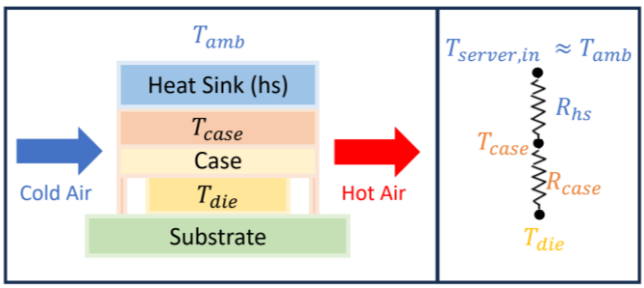

Figure 11. Server Model Schematic with Thermal Resistance [adapted from 27]

Utilization of CPU inside DCs is unique and varies between different types or purposes within DCs itself. Normally it corresponds to the IT workload that is very dynamic, depending on the processed data inside the servers. The available approach to model the CPU Utilization rate can be referred to IT workload schedule which is retrieved from Ham S.W. et al. [27] and applicable to DCs cooling energy prediction according to Central Processing Unit (CPU) utilization.

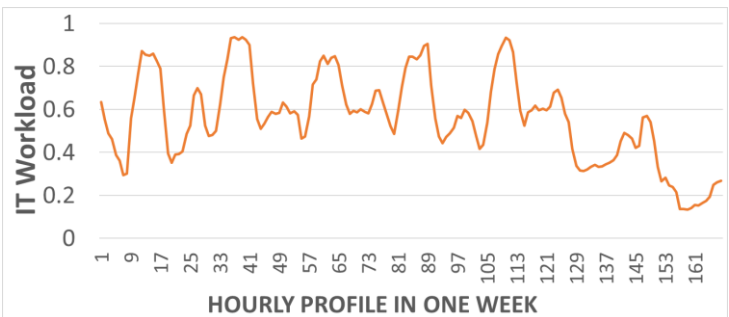

Figure 12. Typical Data Centre Weekly IT workload [reformatted from 27]

Table 1. Measured DCs Performance for Server Model [reformatted from 27]

Ucpu%	**PIT(W)**	**Tdie (°C)**	**Tamb (°C)**	**RPM (RPM)**
10	112.68	54	22.5	1800
50	198.724	70	30	3000
70	211.93	73	35	3600
100	226.508	72	40	9000

All correlated variables such as server internal heat generation (P_{IT}), CPU die Temperature (T_{die}), ambient temperature or server internal air temperature (T_{amb}), and cooling fan rotational speed (RPM) correspond to IT Utilization factor or IT workload (U_{cpu}) as depicted in table 1. Taking into account the above measured performance data, one can conduct regression model to produce the correlation between each of associated variables. The correlation from the measured data is adapted in the way that U_{cpu} is set as the main threshold. The higher U_{cpu}, the higher the associated server temperatures which lead into higher server and cooling fan power. Server power (P_{server}) is the combination of P_{IT} and cooling fan power (P_{sfan}) as written in equation 3 [27].

$$P_{server} = P_{IT} + P_{sfan} \quad \text{(Eq. 3)}$$

P_{IT} calculation is derived as a function of the CPU utilization and CPU die temperature as given in the following equation. The R^2 value of the curve-fitting was 0.9839 [27]. It represents the server heat generation excluding that by the server cooling fan. P_{IT} can be denoted in the equation 4.

$$P_{IT} = 1.57\ x\ 10^{-5} + 42.29\ U_{cpu} + 0.38\ T_{die} + 0.03\ T_{die}^2 \quad \text{(Eq. 4)}$$

Based on given performance data in table 1, one can conduct regression model to produce the correlation in between U_{cpu} with T_{die} and T_{amb}. The R^2 values for these fitted models were 0.9953 and 0.9961 respectively. The related equations are retrieved as equation 5 and 6.

$$T_{die} = -34.42\ U_{cpu}^2 + 58.60\ U_{cpu} + 48.61 \quad \text{(Eq. 5)}$$
$$T_{amb} = 19.74\ U_{cpu} + 20.53 \quad \text{(Eq. 6)}$$

D.Shin et al. [45] defines the server thermal resistance (R_{tot}) as the sum of the heat sink's thermal resistance and the CPU case's thermal resistance. The thermal resistance of a forced-convection heat sink is inversely proportional to the rotational speed of the cooling fan [45]. R_{tot} in this server model is calculated by using an equation retrieved from Ham S.W. et al. [27] in accordance with the difference between T_{die} and T_{amb} divided by P_{IT}. Equation 7 is represented as the function of the server cooling fan RPM via curve-fitting with the R^2 value of 0.935 [27].

$$R_{tot} = \frac{T_{die} - T_{amb}}{P_{IT}} = 0.14 + \frac{17440}{RPM^{1.56}} \quad \text{(Eq. 7)}$$

The server cooling fan power in correlation to the RPM is calculated by using an equation obtained from S. Sampath [43] and denoted as equation 8.

$$P_{sfan} = 7.07\ x\ 10^{-12} RPM^3 - 2.72\ x\ 10^{-8} RPM^2 + 2.61\ x\ 10^{-4} RPM \quad \text{(Eq. 8)}$$

Server outlet temperature T_{server_out} is obtained by the summation of server internal air temperature (T_{amb}) and the server temperature rise (ΔT_{server}). Referred to Ham S.W. et al. [27], server inlet temperature is set 3ºC higher than CRAH supply air temperature, due to absorption of temperature assumed to occur in the ambient from CRAH outlet before cooling the server racks.

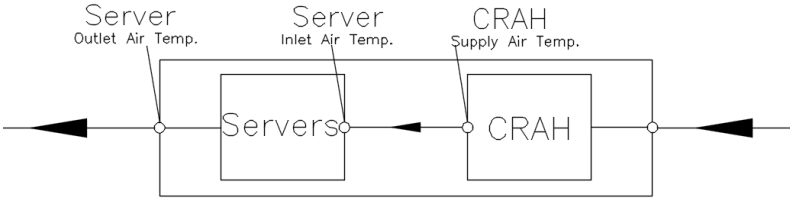

Figure 13. Server Model Workflow to Determine Waste Heat from DCs Air-Cooled System [adapted from 27]

Figure 13 describes the air diagram flow of moving cooled air to server inlet section, before leaving the server itself as a hot air exhaust. T_{amb} is fitted from the measured performance data into the rising server temperature to produce server outlet temperature profile (T_{server_out}) which will then become the input data for waste heat capture (i.e., heat exchange process occurring in hot aisle). The correlation between T_{amb} and ΔT_{server} is obtained from the server heat generation and server inlet air temperature model via curve-fitting with R^2 value of 0.9924, denoted in the following equation 9 [27]

$$\Delta T_{server} = -0.341 T_{amb} + 17.058 \quad \text{(Eq. 9)}$$

Total servers' power ($P_{server\ total}$) is compilation of all server power operated in the whole DC facility. The value corresponds to the number of installed server racks. $P_{server\ total}$ can be written as of this following equation 10.

$$P_{server\ total} = P_{server}\ x\ \sum Server \quad \text{(Eq. 10)}$$

To calculate the number of servers in this thesis work ($\sum Server$), a typical full-size standard rack of 1U is used, in which one 1U can take a total 42 shelves per each 1U modular asset [48]. The nomenclature of 1U standard rack is a typical standard dimension of one server rack with 78 in. of height, 23-25 in. of width and 26-30 in. of depth. Each shelf has two servers. With

assumption of 150 server racks installed in DC facility, there're 150 x 42 x 2 = 12,600 servers in total for this thesis work. The IT power rating of those 12,600 servers represents medium-to-large scale commercial DCs in Stockholm [49,50].

3.2.2 DC Cooling System

The DC cooling power model is adopted from the modular simulation of DC power load proposed by R. Rahmani et al. [22] which provides hourly power consumption profile for cooling system. Cooling power consumption in the model consists of both CRAH (P_{CRAH}) and Chiller plant ($P_{chiller}$). Chiller and CRAH system depend on IT equipment operation. It acts as the main factor that causes servers to produce more heat or less heat, which affects the computer room air temperature [22]. The higher the IT utilization factor (U), the bigger the cooling consumption to cool down the server racks. $P_{chiller}$ as U function can be denoted as of this following equation 11.

$$P_{chiller} = 0.7\ x\ P_{sf}^{max}\ x\ (\alpha\ \mathrm{U}^2 + \beta\ \mathrm{U} + \gamma) \quad \text{(Eq. 11)}$$

Constant coefficient values are α = 0.32, β = 0.11, and γ = 0.63, referring to the curve fitting values conducted by R. Rahmani et al. [22]. For medium to big size DC (>100 kW) the use of CRAH is preferable due to its lower operational costs in comparison with CRAC solutions [24]. Hence, CRAH system is chosen in this model due to its size compatibility to provide cooling for the given server rack power rating in the model (i.e., 20.6 kW of IT power per rack, or >3MW for given total server racks), while in contrast CRAC is normally used in small DCs (<100 kW) due to lower capital costs [24]. The electrical power consumption for heat transfer to be consumed by an air handling system (P_{heat}) for a server farm with maximum server load of P_{sf}^{max} can be derived from these following equations 12 and 13 [22].

$$P_{heat} = 1.33\ x\ 10^{-5}\ x\ \frac{P_{sf}^{max}}{\eta_{heat}}\ x\ f \quad \text{(Eq. 12)}$$

$$f = f^{max}\ x\ U \quad \text{(Eq. 13)}$$

P_{sf}^{max} is an operational state of the total server racks (i.e., in other words can be called as server farm), which is the maximum value of $P_{server\ total}$ defined in the equation 10 before. η_{heat} describes the efficiency of heat removal from the system. On the other hand, the power consumption required for heat cycling is linearly proportional to the volume of the air flow (f) with f^{max} as the maximum standard air flow. Finally, total power requirement of CRAH unit (P_{CRAH}) can be calculated as of this following equation 14.

$$P_{CRAH} = P_{CRAH}^{idle} + P_{heat} \quad \text{(Eq. 14)}$$

P_{CRAH}^{idle} is CRAH power consumption in idle mode, ranging from 7 to 10 percent from P_{sf}^{max}[22].

3.2.3 DC Free Cooling System

Free cooling system in this work uses Indirect Air Side Economizer (IASE) model adapted from Park S. et al. [38]. The heat exchange between outdoor temperature (T_{OA}) and the return air from DC exhaust (T_{RA}) generates the secondary return air (T_{RA*}) which can be formulated in the following equations 15 and 16 [38]. The T_{RA} temperature passing through heat exchanger becomes closer to the T_{OA} which has lower temperature than T_{RA} during wintertime, and that can lead into lower cooling energy that would otherwise require CRAH to generate the desired cold air supply temperature with chilled water.

$$T_{RA*} = T_{RA} + \varepsilon\, HX_{flow\,ratio} \left(\frac{\dot{m}_{OA}}{\dot{m}_{RA}}\right) x\, (T_{OA} - T_{RA}) \quad \text{(Eq. 15)}$$

$$HX_{flow\,ratio} = (\dot{m}_{OA} + \dot{m}_{RA})/2\dot{m}_{RA} \quad \text{(Eq. 16)}$$

T_{OA} as initial set point defines the operation plan of IASE system in the way that free cooling will be operated when T_{RA*} doesn't exceed the temperature of cold air supply to DC server racks (T_{SA}). In this model, T_{SA} is set at maximum 20ºC. If T_{RA*} doesn't meet T_{SA} criteria (especially during summer due to higher outdoor temperature), the CRAH cooling system will be activated to help provide the desired cooling needs to DC servers. In configuration A2, the T_{RA} for free cooling model input refers to the exhaust temperature resulted from the server racks; while in configuration A4, T_{RA} is the outlet temperature after waste heat recovery in the heat exchanger (T_{RA_out}). The schematic diagram of the free cooling system can be seen in the following figure 14.

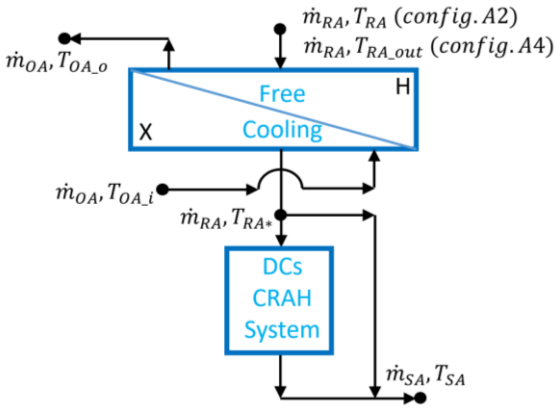

Figure 14. DC Free Cooling Schematic Diagram

3.2.4 DC Waste Heat Capture

In case of air-cooled DCs system, the waste heat recovery from the outlet server temperature through hot aisle is modelled with zero capacitance sensible heat exchanger model [28]. Given two input parameters which are both mass flow rate and inlet temperatures of hot and cold sides, the other outlet parameters can be estimated by the principle of heat exchanger effectiveness for a fixed value of overall heat transfer coefficient. Waste heat from DC is the hot inlet side of the heat exchanger while the cold side input refers to the outlet of evaporator heat source, and both are used as preliminary input parameters. The schematic diagram of the DC waste heat recovery process is depicted in the figure 15.

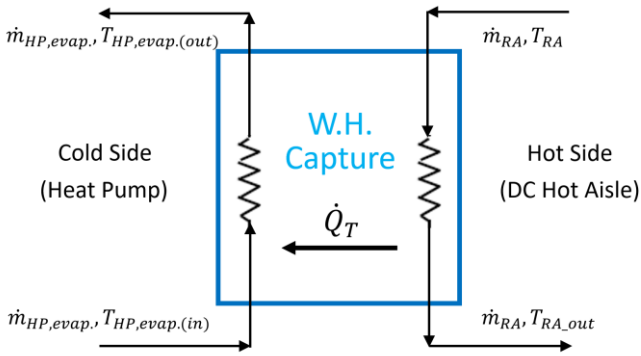

Figure 15. Heat Exchanger model for DC WHR

Using cross flow heat exchange with both sides unmixed model adapted from [28], the heat exchange effectiveness (ε) can be written as of these following equations 17 and 18. The effective heat exchange area (A) used is 38 m² with

the overall heat transfer coefficient (U) of 500 W/m² K adapted from Dimian A.C. et al. [53] for the air-cooled heat exchanger model with water cooling.

$$\varepsilon = 1 - \exp\left[\left(\frac{C_{max}}{C_{min}}\right)\left(\frac{UA}{C_{min}}\right)^{0.22}\left\{exp\left[-\frac{C_{min}}{C_{max}}\left(\frac{UA}{C_{min}}\right)^{0.78}\right]-1\right\}\right] \quad \text{(Eq. 17)}$$

$$If\ \frac{C_{min}}{C_{max}} \leq 0.01,\ then\ \varepsilon = 1 - \exp\left(-\frac{UA}{C_{min}}\right) \quad \text{(Eq. 18)}$$

The outlet temperature of the hot side (T_{RA_out}) will depend on ε, minimum capacity rate (C_{min}), capacity rate of fluid on hot side (C_{RA}), and the inlet temperatures of both hot and cold sides (T_{RA} and $T_{HP,evap.(in)}$ respectively). The value of T_{RA_out} can be calculated as of the following equation 19 [28].

$$T_{RA\_out} = T_{RA} - \varepsilon\left(\frac{C_{min}}{C_{RA}}\right)\left(T_{RA} - T_{HP,evap.(in)}\right) \quad \text{(Eq. 19)}$$

The dynamic value of T_{RA_out} will be the main input parameter for the cooling model as mentioned in the previous sub-chapters 3.2.2 and 3.2.3, applicable to both system configuration of WHR without free cooling (configuration A3) and WHR with free cooling (configuration A4). The total heat transfer rate ($\dot{Q}_T$) across heat exchanger can be denoted as per following equation 20 [28].

$$\dot{Q}_T = \varepsilon\, C_{min}\left(T_{RA} - T_{HP,evap.(in)}\right) \quad \text{(Eq. 20)}$$

3.2.5. DC Waste Heat Upgrade

DC waste heat upgrade is done with heat pump. The heat pump simulation complies with COP Carnot principle, taking into accounts all sub-components of the heat pump. The heat pump system acquires given temperatures as input parameters to determine the energetical values in each time step. The energetic parameters in heat pump modelling include evaporation pressure of chiller ($P_{Evap\_chiller}$), enthalpy of evaporation outlet (H_{Evap_out}), enthalpy of suction ($H_{Suction}$), entropy of suction ($S_{Suction}$), condensation pressure (P_{Cond}), enthalpy of isentropic discharge ($H_{Discharge\_is}$), and enthalpy of heat sink (H_s). The temperatures between components and the enthalpy of the refrigerant in each state are determined with CoolProp library [29]. The evaporating temperature of heat pump is associated with superheat temperature to ensure the refrigerant gets boiled before entering the compressor. Upon calculating associated enthalpies inside evaporator, one can calculate mass flow rate of chiller ($\dot{m}_{chiller}$) with this following equation 21.

$$\dot{m}_{chiller} = \frac{\dot{Q}_{DC\_cooling}}{H_{evap\_out} - H_s} \quad \text{(Eq. 21)}$$

DC cooling power ($\dot{Q}_{DC\_cooling}$) in this case refers to thermal cooling power to cool down data server racks. Its value depends on the difference between inlet air temperature going to server racks (i.e., T_{SA}) and the exhaust air temperature coming out from the server racks ($T_{server,out}$). $\dot{Q}_{DC\_cooling}$ can also be written as per following equation 22.

$$\dot{Q}_{DC\_cooling} = \dot{m}_{cooling}\ x\ C_{p,air}\ x\ (T_{SA} - T_{server,out}) \quad \text{(Eq. 22)}$$

Lifting heat quality will require additional power, that is fed through compressor heat pump. The compressor efficiency is constant, assuming isentropic condition in the compression process. The DH temperature is applied in the model as boundary condition to define heat pump parameters for P_{Cond}, $H_{Discharge\_is}$, and H_s. The higher the waste heat source temperature from DC server outlet racks, the lower compressor power needed to boost the heat sink desired temperature, in this case to produce designated warm water for DHN. Compressor power in each time step ($P_{HP.,comp.}$) is the net energy needed by heat pump system, which can be determined from this following equation 23.

$$P_{HP.,comp.} = \frac{\dot{m}_{chiller}\ x\ (H_{Discharge\_is} - H_{Suction})}{\eta_{comp.}} \quad \text{(Eq. 23)}$$

The upgraded waste heat profile from data centre is in accordance with the district heating temperature profile in DHN. The amount of waste heat that is injected to DHN ($\dot{Q}_{DH}$) can be denoted as per following equation 24:

$$\dot{Q}_{DH} = \dot{Q}_{DC\_cooling} + (P_{HP.,comp}\ \eta_{supp,DH}) \quad \text{(Eq. 24)}$$

The efficiency of heat supply to DHN ($\eta_{supp,DH}$), is assumed to be 0.97, meaning that around 3% of hourly loss during heat transmission to DHN is considered. On the other hand, Coefficient of Performance (COP) of the heat pump is defined as total heat injected to DHN divided by compressor power to drive the heat pump itself. The amount of heat injected to DHN ($\dot{Q}_{DH}$) corresponds to heat production in the heat pump condenser (i.e., heat sink). The COP value refers to the following equation 25.

$$COP = \frac{\dot{Q}_{DH}}{P_{HP.,comp.}} \quad \text{(Eq. 25)}$$

3.3 Key Performance Indicators (KPIs)

KPIs in this thesis work encompass two main parameters, namely technical KPIs and economic KPIs. It will reveal results which will be analysed in the next chapter.

3.3.1 Technical KPIs

Metrics to measure data centre performance have gone beyond the DCs facility power and its cooling system and have been used by data centre industry [32]. DCs acting as prosumers must consider both production and consumption of their scoped energy systems. In the context of DC energy system and waste heat utilization, three parameters will be considered, namely Power Usage Effectiveness (PUE), Energy Reuse Factor (ERF), and Energy Reuse Effectiveness (ERE).

PUE gives an understanding on how energy is consumed for all systems within the data centre, cooling, power distribution, and other ancillary systems [32]. The PUE itself has no correlation directly with waste heat utilization. PUE as a mathematical formula can be written as per following equation 26.

$$PUE = \frac{\dot{E}_{DC,tot}}{\dot{E}_{IT}} \quad \text{(Eq. 26)}$$

Total power consumption in data centre ($\dot{E}_{DC,tot}$) denotes an accumulation of associated total power consumed for IT equipment ($\dot{E}_{IT}$), total cooling system ($\dot{E}_{cooling,system}$), and total auxiliary system ($\dot{E}_{Aux.}$). For system configuration A3 and A4 however, the $\dot{E}_{DC,tot}$ also includes the electrical power to drive heat pump compressor ($\dot{E}_{HP.,comp.}$) as the waste heat needs to be upgraded before being injected to DHN. $\dot{E}_{Aux.}$value represents all miscellaneous power consumption such as lighting, network equipment, control, and protection devices. $\dot{E}_{Aux.}$ is normally valued at 6% of DC peak power demand [42]. $\dot{E}_{IT}$ value is the total IT equipment power consumption of DC servers and adhered to previously discussed chapter 3.2.1.

To be noted hereby, the $\dot{E}_{cooling,system}$ is the total associated electrical power of cooling consumption, which varies according to the applicable equations mentioned in sub-chapter 3.2.2 and 3.2.3 before. $\dot{E}_{cooling,system}$ in configurations A1 and A3 are the power consumptions of both CRAH and Chiller. On the other hand, in configurations A2 and A4, the free cooling model is included as part of the system configuration scope. The equations for total DC power consumption ($\dot{E}_{DC,tot}$) for configurations A1 and A3 can be written as of equations 27a and 27b.

$$\dot{E}_{DC,tot(for\ A1)} = \dot{E}_{IT} + \dot{E}_{Aux.} + \dot{E}_{cooling,system(for\ A1)} \quad \text{(Eq. 27a)}$$

$$\dot{E}_{DC,tot(for\ A3)} = \dot{E}_{IT} + \dot{E}_{Aux.} + \dot{E}_{cooling,system(for\ A3)} + P_{HP.,comp.} \quad \text{(Eq. 27b)}$$

The equations for total DC power consumption ($\dot{E}_{DC,tot}$) for configurations A2 and A4 can be written as of equations 28a and 28b.

$$\dot{E}_{DC,tot(for\ A2)} = \dot{E}_{IT} + \dot{E}_{Aux.} + \dot{E}_{cooling,system(for\ A2)} \quad \text{(Eq. 28a)}$$

$$\dot{E}_{DC,tot(for\ A4)} = \dot{E}_{IT} + \dot{E}_{Aux.} + \dot{E}_{cooling,system(for\ A4)} + P_{HP.,comp.} \quad \text{(Eq. 28b)}$$

ERF on the other hand has been used by DCs industry and standardization to quantify external waste heat utilization [30]. ERF is a ratio of energy reused divided by the sum of all energy consumed in data centre. ERF is used to quantify the external waste heat usage of data centre and can be formulated as per following equation 29.

$$ERF = \frac{\dot{Q}_{DH}}{\dot{E}_{DC,tot}} = \frac{\dot{Q}_{DH}}{\dot{E}_{IT}\ x\ PUE} \quad \text{(Eq. 29)}$$

Key assessment for ERF has lower end of zero when no heat is reused, and the upper end of 1 when all the waste heat is reused (i.e., $\dot{Q}_{DH}$ equals to $\dot{E}_{DC,tot}$). The higher ERF value, the better the performance metrics to consider WHR effectiveness from DC. The results will be discussed in the next chapter.

On the other hand, ERE was developed to recognize DCs ability to provide energy that can be reused, for instance heat service to adjacent buildings or domestic hot water pre-heating [32]. ERE is the ratio of the difference between total DCs facility energy use and energy reused, divided by IT energy use. ERE metrics can be formulated as of this following equation 30:

$$ERE = \frac{\dot{E}_{DC,tot} - \dot{Q}_{DH}}{\dot{E}_{IT}} = (1 - ERF)\ x\ PUE \quad \text{(Eq. 30)}$$

Both ERF and ERE are direct performance metrics to include the amount of energy reused in the form of waste heat utilization from DCs.

In this thesis work, additional indicators are proposed to analyse the value of energy reused from DC's associated power consumption, in the context of

waste heat upgraded. Those indicators are assigned as Seasonal Performance Factor (SPF) and Heating Seasonal Performance Factor (HSPF). SPF is developed into two different categories, namely SPF in correlation with DC thermal power ($SPF_{thermal}$), and SPF in comparison with IT power (SPF_{IT}), which can be written as of these following equations 31 and 32.

$$SPF_{thermal} = \frac{\dot{Q}_{DH}}{\dot{E}_{DC,tot} - \dot{E}_{IT}} \quad \text{(Eq. 31)}$$

$$SPF_{IT} = \frac{\dot{Q}_{DH}}{\dot{E}_{IT}} \quad \text{(Eq. 32)}$$

As part of Heat Pump's KPI, HSPF in the context of ODH heat supplier will be defined as the output of thermal energy delivered to the ODH network compared to the input of electricity needed to run the heat pump's compressor. The HSPF equation can be formulated as of following equation 33.

$$HSPF = \frac{\dot{Q}_{DH}}{P_{HP,comp.}} \quad \text{(Eq. 33)}$$

The results of those parametric numbers (i.e., PUE, ERF, ERE, SPFs, and HSPF) will enrich the discussions of each of different scenario tested, to support the decision-making whether WHR from DC is a favourable investment or not.

3.3.2 Economical KPIs

The main economical KPI used in this thesis for economical assessment is operational expenditure (OPEX) related to energy that is both consumed and produced. Since most DC operations are not public, using OPEX as the economical measurement is decided for this thesis work, which can still determine the profitability of different system configurations in DC facility. OPEX is determined as total associated energy costs of each given system configuration. Since there is WHR in both configurations A3 and A4, the related OPEX also includes energy cost to drive heat pump compressor while considering the energy output injected to DHN. The parameter will help investigate the trade-off between electricity price ($C_{elec.}$) and DH price (C_{DH}) that demonstrates for how beneficial the monetary value of selling heat to DHN can offset the heat pump operational expenditure. Both $C_{elec.}$ and C_{DH} vary hourly (t). The equation to determine OPEX in hourly values can be denoted as of this following equation 34.

$$OPEX_{(t)} = [(\dot{E}_{IT(t)} + \dot{E}_{Aux.(t)} + \dot{E}_{cooling(t)} + P_{HP.,comp.(t)})\ x\ C_{elec.(t)}] - [\dot{Q}_{DH(t)}\ x\ C_{DH(t)}] \quad \text{(Eq. 34)}$$

The discount rate (r) is included in the calculation as part of time value of money. Since the inflow and outflow are discounted and netted out yearly (i) without capital expenditure (CAPEX), the sum of it refers to Life Cycle OPEX (LCO) which can be written as equation 35.

$$LCO = \sum_{i=1}^{n} \frac{OPEX}{(1+r)^i} \quad \text{(Eq. 35)}$$

LCO represents the maximum CAPEX that data centre should accept when recovering the waste heat to the DHN. The system configuration with lower OPEX is deemed more interesting or more profitable. Lower OPEX means less burdened costs that are included in the financial operability of DC, leading to overall operational cost saving.

3.4 Heat Supply Scenario

Scenario development for the upgraded waste heat intends to obtain in-depth understanding of complexity between electricity price and outdoor temperature applied to the model. The correlation curve between outdoor temperature and DHN temperature is obtained from C. Mateu-Royo et al. [46] which is shown in figure 16. Five cases for DHN supply temperatures are developed to obtain the relationship on how it affects the amount of heat supplied from DC's WHR to the DHN. The DHN supply temperature is utilized as the target temperature for WHR model in the previous sub-chapters and varied into low case and high case from the baseline. The baseline case for supply temperature to ODH network is delivered at 68-103 ºC following the requirement by Stockholm Exergi [5]. The other four cases are denoted as low, low-medium, medium-high, and high cases which correspond to the different supply temperature level but having the same minimum temperature of 68 ºC which is also adhered to the minimum temperature to prevent the growth of legionella bacteria.

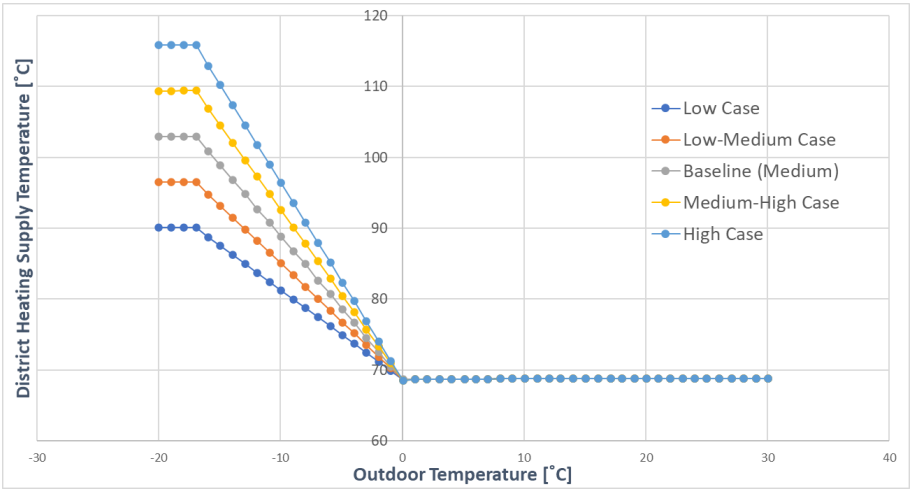

Figure 16. DHN Temperature used in the model [reformatted from 46]

On the other hand, the price curve model of the correlation between outdoor temperature and DHN price is retrieved from Fabio G., et al. [26] which can be depicted in the following figure 17.

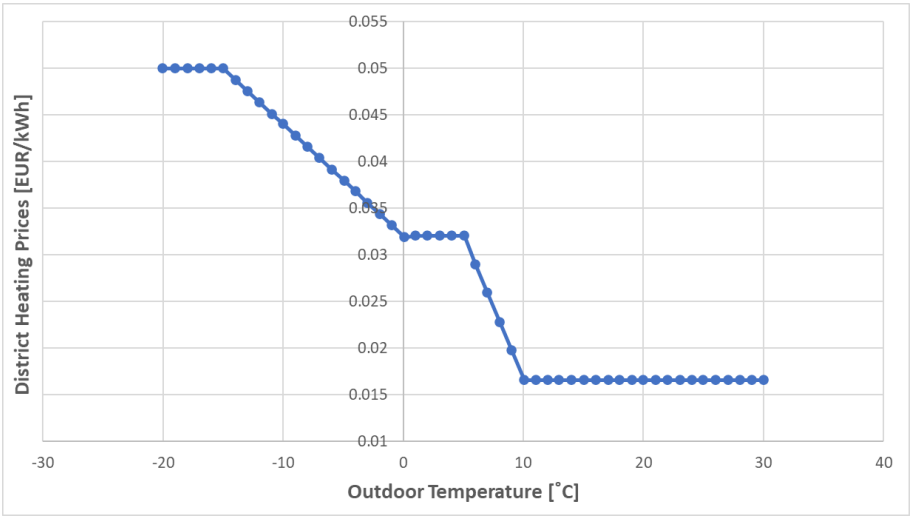

Figure 17. DHN Price used in the model [adapted from 26]

The upgraded waste heat ($\dot{Q}_{DH}$) from previous sub-chapter 3.2.5 is examined into three different scenarios. The first scenario is called "All-Heat" and set as benchmark, which is exactly the available amount of waste heat from DC servers that is upgraded by the heat pump. The second scenario is denoted as "Market-Limit" and adhered to the requirement stated by Stockholm Exergi, in which heat injection to DHN occurs when the outdoor temperature is 12 ºC or below [5]. The third scenario is called "Price-Limit" and proposed for certain

condition that there will be heat injection to DHN when the revenue of selling the heat to DHN is positive. It means that DC owners will only supply their upgraded waste heat whenever heat remuneration can offset the electricity cost required to operate the heat pump, otherwise there will be no heat injection to DHN.

Hourly Electricity price data applicable for Stockholm Region is taken from NordPool [36]. The historical five-consecutive years of electricity prices are adopted in the model from 2018 until 2022. Outdoor temperature is obtained from Meteonorm [37], with dataset refined in four different climate conditions in Stockholm Region. Typical Metrological Year (TMY) is set as benchmark of climate condition using the years 2000-2019 as data source. The remaining three conditions are based on Intergovernmental Panel on Climate Change (IPCC) with Representative Concentration Pathways (RCP). Referring to the abbreviation numbers of each RCP indicated by World Bank [44], it represents RCP2.6 (Low Condition), RCP4.5 (Mid Condition), and RCP8.5 (High Condition). Each RCP path represents future climate change scenario, and all of which are thought to be conceivable depending on the amount of greenhouse gases (GHG). Those RCP values are refined hourly for 2050 scenario and aimed to obtain in-depth understanding on how the tendency of rising global temperature due to climate change scenario will affect the heat supply model to DHN.

4. Results

The results are presented in four sections; the data centre energy consumption, the waste heat recovered to DHN, technical KPIs, and economic KPIs.

4.1 Data Centre Energy Consumption

Data centre runs continuously all year round according to their associated energy consumptions; cooling energy, IT Equipment, and auxiliaries (such as security, network conditioning, etc.). The result of monthly energy consumption of DC running in BaU scheme (i.e., configuration A1 as baseline) can be depicted in the Figure 18.

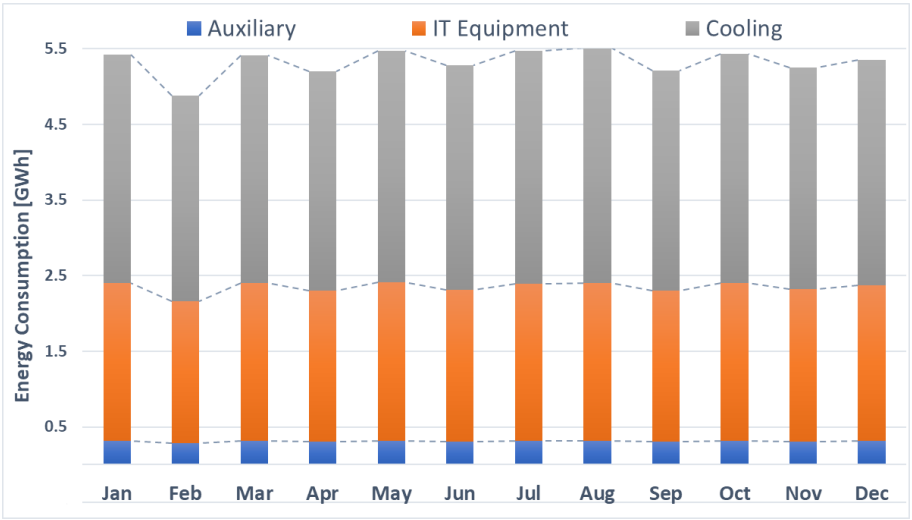

Figure 18. Distribution of Energy Consumption in BaU Data Centre

The cooling power follows the pattern of the IT power consumption which is dependent on the IT utilization workload. In such case, when the IT workload increases, the cooling air supply is also increased, following the demand. The cooling consumption in February is lower than for instance in January because in February there're 28 days while January has 31 days. It can be also refined from figure 19 that the cooling energy in configuration A1 constitutes to the largest portion of the annual energy consumption, measured at 35.73 GWh (i.e., 55.8% from total DC consumption). Cooling energy in an inefficient DC energy system contributes to more than a half of the DC's total energy consumption [56, 59]. Remarkably, reducing cooling consumption is critical to achieve an efficient DC energy system. In fact, the cooling consumption in configuration A1 is operated without considering both FC and WHR. The

comparison of cooling consumption in different system configurations is demonstrated by the following figure 19.

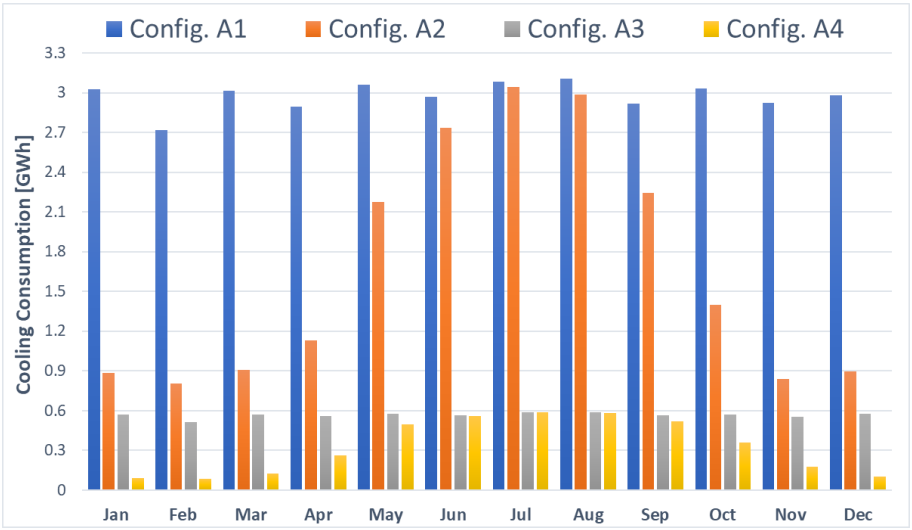

Figure 19. Comparison of Cooling Consumption in Different Configurations

When comparing cooling consumption within different configurations, configuration A1 is the least efficient. When FC is included in configuration A2, the annual cooling consumption is reduced by 43.91% to 20.04 GWh. During wintertime when the outdoor temperatures are low, the monthly reduction can reach 69.8% (i.e., in December, from 2.97 GWh to 0.89 GWh). Mostly in summertime, FC system can't accommodate the demand to supply cold air to DC which results in the higher energy consumption following the baseline. On the other hand, configuration A3 has much lower and constant cooling power compared to configuration A1 and A2. With the WHR included in configuration A3, the inlet temperature going into CRAH system becomes lower due to the heat exchange from waste heat capture (i.e., T_{RA} becomes T_{RA_out} and T_{RA_out} is lower than T_{RA}). It's worthwhile to note that the cooling consumption in configuration A3 is based on the WHR model explained in subchapter 3.2.4. In that case, the heat capture model converts T_{RA_out} into its highest temperature drop which is nearly the same with T_{SA} before going into CRAH. With the return air entering CRAH being closer to supply air temperature, the lower energy consumption in the CRAH can be accomplished because the energy needed to produce chilled water in the CRAH system to cool down the return air is also lower.

The cooling power consumption in figure 19 is applied with the same baseline temperature (i.e., TMY profile) for each configuration. To provide more contexts on how the outdoor temperatures influence the cooling power

consumption, configuration A2 is examined with four different climate conditions as of figure 20.

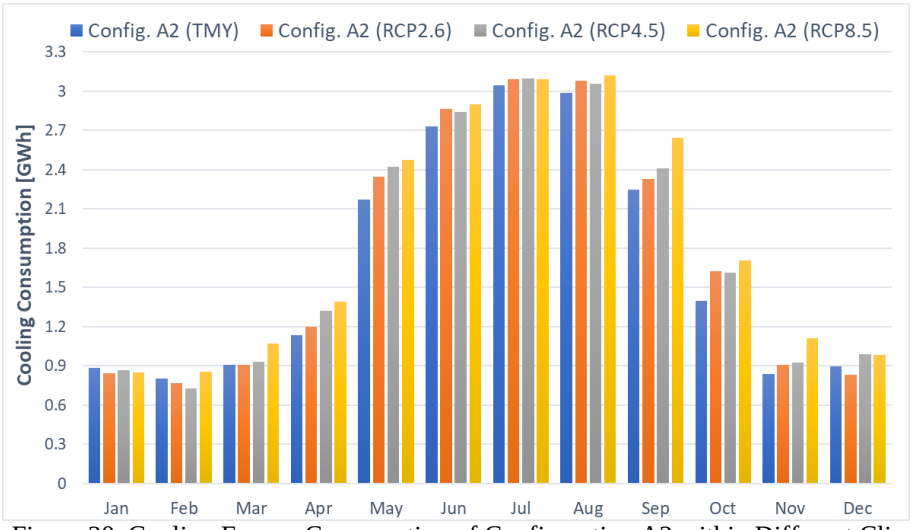

Figure 20. Cooling Energy Consumption of Configuration A2 within Different Climate Conditions

As can be seen in figure 20, the same monthly pattern of FC system occurs in each climate condition, being always lower in the wintertime than summertime. The climate condition in RCP8.5 shows the highest cooling consumption compared to TMY, RCP2.6, and RCP4.5. The worst climate condition (i.e., RCP8.5) has the highest rising temperature, leading to higher cooling consumption to compensate such higher outdoor temperature. Annual cooling energy consumption of configuration A2 in RCP8.5 condition is measured at 22.2 GWh, compared to 20.04 GWh in TMY condition. Considering this result, the effect of climate change is existed to DC cooling system but not significant. The distribution of annual cooling energy consumption for each configuration can be summarized in the figure 21 which is plotted in the same climate condition (i.e., TMY).

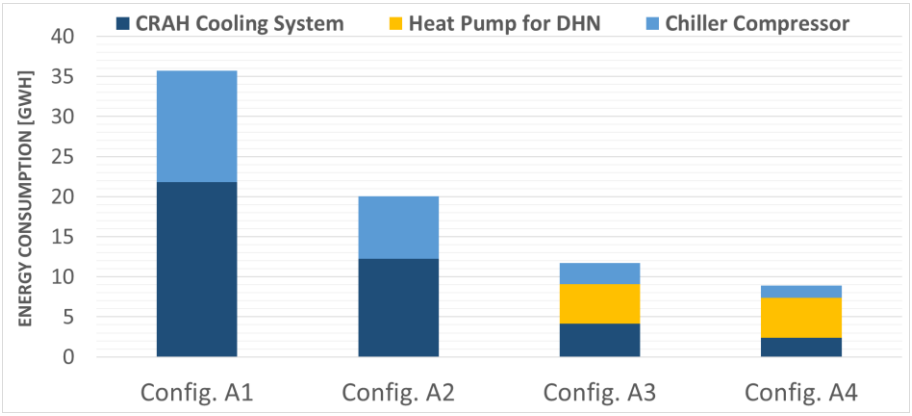

Figure 21. Summary of Annual Cooling Energy Distribution within Each Configurations

From figure 21, one can see a significant reduction in both chiller and CRAH consumption by moving away from configuration A1. The greatest reduction is observed in configuration A4. Waste heat from CRAH's cooling energy is recovered in configuration A3 and A4, saving significant amount of cooling energy. With FC included in the system, further reduction can be accomplished by configuration A4 in saving CRAH cooling energy.

The annual cooling energy reduction in configuration A3 reaches 67.14% from the configuration A1 as the baseline (i.e., from 35.73 GWh to 11.74 GWh). Furthermore, it can be also seen that the combination of WHR and FC in configuration A4 generates the lowest cooling consumption among all configurations. Cooling consumption in configuration A4 peaks during summertime and reaches the equivalent consumption with configuration A3 due to such high outdoor temperature which prevents free cooling system to supply the desired cold air to DC servers. By using configuration A4, the annual cooling energy from the baseline can be further decreased by 75.1% to 8.89 GWh. On one specific hand, configuration A2 with free-cooling mode can be deemed typical in Sweden (i.e., taking advantage of cold climate outdoor temperature). Accordingly, when the comparison is made from the perspective of configuration A2, the reduction of cooling consumption by transitioning from configuration A2 to A4 will reach 55.61% (from 20.04 GWh to 8.89 GWh).

4.2 Waste Heat Recovered to DHN

The reduction of cooling energy in configuration A3 and A4 is achieved by waste heat recovery system in the hot aisle compartment of DC's server racks. The recovered cooling waste heat in configuration A3 and A4 is boosted by

heat pump before being supplied to the DHN. The annual heat pump energy is measured at 4.95 GWh while the recovered cooling energy from the CRAH stands at 17.65 GWh. The monthly heat supply profile to DHN for each heat supply scenario can be seen in figure 22.

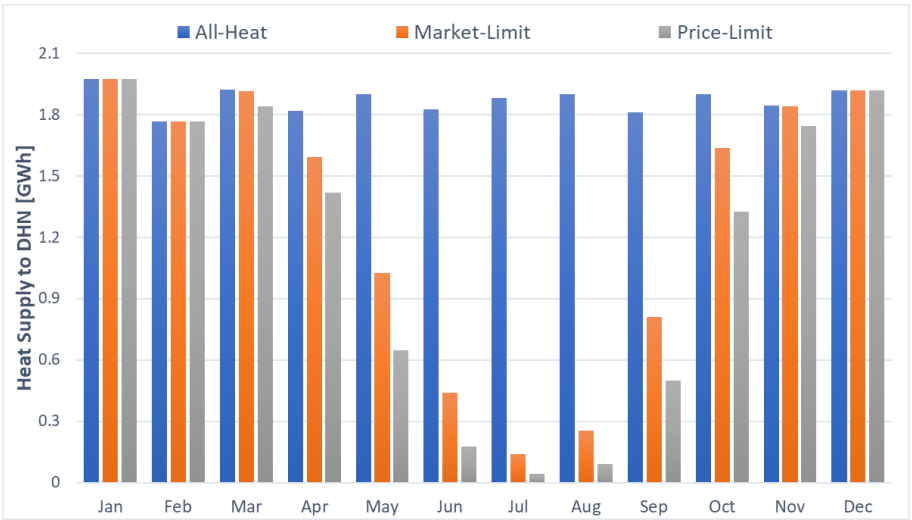

Figure 22. Heat Supply to DHN within Different Heat Supply Scenarios

All-Heat supply scenario demonstrates the highest heat supply compared to Market-Limit and Price-Limit with annual waste heat supply of 22.45 GWh. It can be explained because all recovered waste heat can be injected to DHN with All-Heat. In Market-Limit, the DC owners are constrained to specific condition as they are only allowed to supply heat to DHN when the outdoor temperature is 12ºC or below, while in Price-Limit, the DC owners will only supply heat if the revenue of selling heat is positive. Lower heat supply to DHN occurs during summertime for both Market-Limit and Price-Limit. For instance, the heat supply in June with Market-Limit can only reach 0.43 GWh or around 24% from its original waste heat of 1.82 GWh. This can be explained as higher outdoor temperatures during summertime which cause lower heat demand in DHN supply line. This specific amount, however, is still higher than Price-Limit in the same month, which only stands at 0.178 GWh. Low heat supply in Price-Limit occurs also during summertime because the revenue of selling heat during low demand can't offset the electricity cost to drive the heat pump compressor. The heat price in higher outdoor temperature (i.e., summertime) is also lower than wintertime as it can be seen from previous figure 17. Hence at the same time, it's not profitable should DC owners sell the heat with lower revenue while absorbing electricity from the grid is also costly. During wintertime when the heating demand is at its peak, almost all DC waste heat can be injected to DHN. It can be seen for instance in December, January, and February where heat supplies in both Market-Limit and

Price-Limit can reach its maximum from the available waste heat from All-Heat.

It is worthwhile to note that the heat supply profile depicted in figure 22 depends solely on the same climate condition and electricity price. The relationship between different climate conditions and how it affects the heat supply to DHN can be demonstrated by the following figure 23.

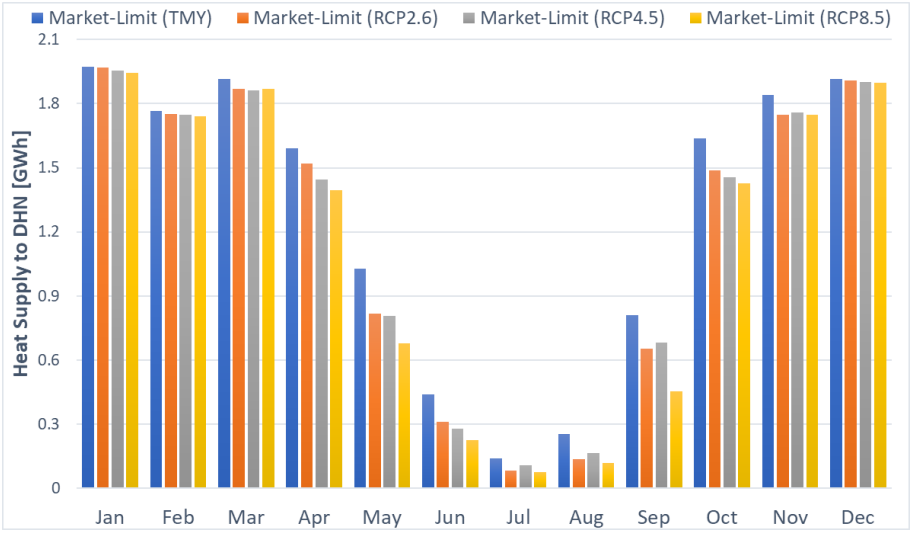

Figure 23. Heat Supply to DHN of Market-Limit within Different Climate Conditions

As it is also expected from figure 23, the effect of climate change doesn't contribute significantly to the accumulation of heat supply in general. Annual heat supplies of each climate condition are calculated 15.31, 14.26, 14.17, and 13.57 for TMY, RCP2.6, RCP4.5, and RCP8.5 respectively. However, it's still worthy to emphasize that there's still a variation of heat supply comparing the different climate condition. The lowest heat supply with climate condition RCP8.5 is obtained, particularly during summertime due to its highest outdoor temperature. RCP8.5 in comparison with TMY possesses lower heat supply because of the higher outdoor temperature that causes lower temperature in DH supply network. Most of the wintertime though, each climate condition injects almost the same amount of heat. After wintertime, it then starts declining from spring to summertime with the different trendline profile seen on each climate condition. For instance, in May, the RCP8.5 is measured at 0.68 GWh which is 34% lower than TMY of 1.03 GWh. From the result, it can be refined that the higher the outdoor temperatures (i.e., the higher climate condition), the lower the amount of heat supply to the DHN even though the amount isn't too significant annually.

On one specific hand, the other variable tested is the difference in electricity price which also influences the heat supply to DHN according to Price-Limit scheme. The presence of electricity on how it affects the heat supply can be referred to figure 24.

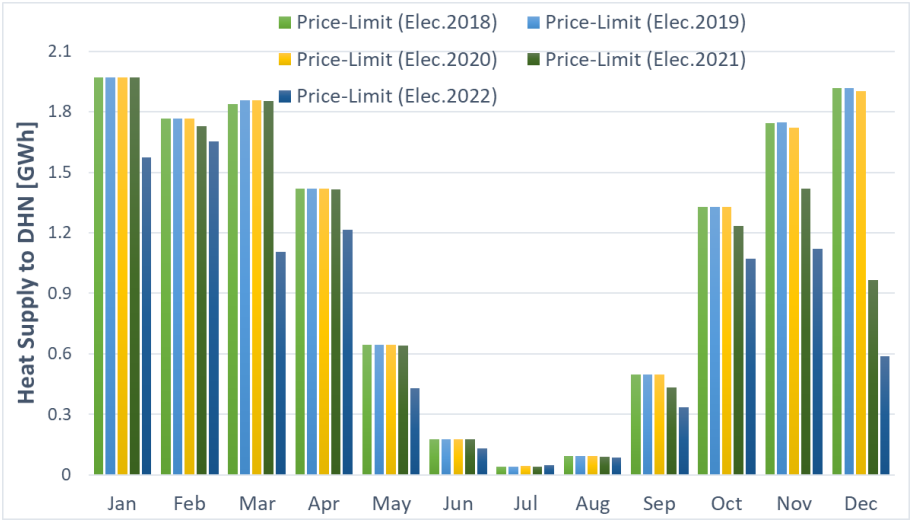

Figure 24. Heat Supply to DHN of Price-Limit within Different Electricity Prices

It's important to note that the Price-Limit supply as in figure 24 is plotted in accordance with the same climate condition. By utilizing 5 historical electricity data as the changing variable, the monthly pattern of heat supply also follows the same seasonal behaviour, in which during summertime the supply is lower compared to wintertime. However, the annual amount of supplied heat varies significantly within different applied electricity prices. For instance, it turns out that should the heat pump be operated using electricity in 2022, the annual heat supply to DHN will drop by 58.3%, from 22.45 GWh (as per All-Heat scenario or baseline) to only 9.36 GWh. This Price-Limit scenario based on 2022 electricity result can be compared for example, with the heat supply following electricity price of 2019, at which the annual heat supply can reach 13.46 GWh. The annual average wholesale electricity prices were in fact 460.88, 406.75, 221.28, 671.61, and 1382.12 SEK/MWh for all five consecutive years (i.e., from 2018 until 2022 respectively) [36]. The annual average wholesale electricity price in 2022 is much higher than in 2019. In other words, the higher the electricity price, the lower the heat supply if one should consider supplying heat to DHN with Price-Limit. Furthermore, this result clearly informs that electricity price has greater impact than the climate condition in terms of influencing the amount of heat supply to DHN. To capture the understanding of correlating both variables (i.e., electricity price and climate condition) at the same time, figure 25 sums up the annual heat supply for all scenarios.

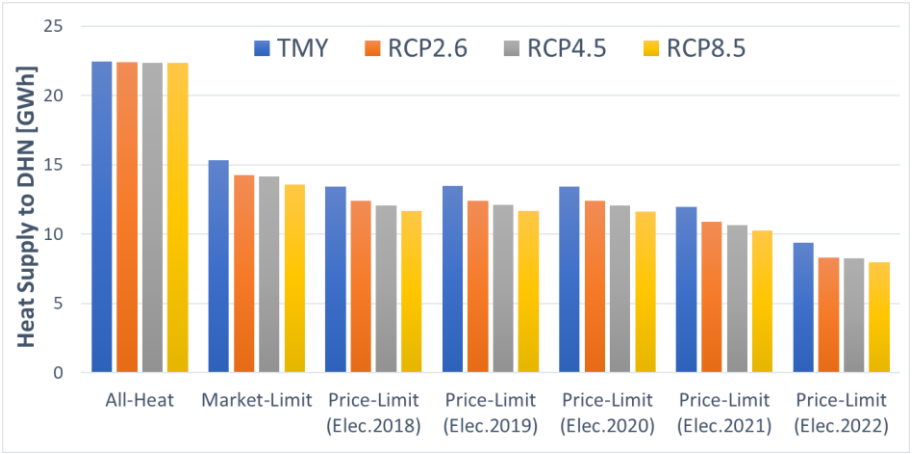

Figure 25. Summary of Annual Heat Supply to DHN within applicable climate conditions and electricity prices

Price-Limit in figure 25 is developed to such extent should the heat supply be based on different climate conditions, while Market-Limit is originally set according to previous explanation. All-Heat has very minor influence with different climate conditions as the heat supply is based upon IT equipment workload in the server racks. Oppositely, there's an influence on raising outdoor temperatures which can be demonstrated by Market-Limit and Price-Limit. Both heat supply scenarios when tested with different climate conditions clearly show the decreasing trendline from low average outdoor temperature (i.e., TMY) to higher average outdoor temperature (i.e., until RCP8.5). For instance, the annual heat supply in Market-Limit stands at 15.31 GWh with TMY condition before declining by 12.7% to 13.57 GWh with RCP8.5 condition. Price-Limit by using electricity data of 2018 also demonstrates the decrease by 15.3% in heat supply from 13.44 GWh with TMY condition to 11.65 GWh with RCP8.5 condition. This phenomenon shows that the higher the outdoor temperature, the lower the annual heat supply to DHN within Market-Limit and Price-Limit.

On the other hand, electricity price plays more significant roles in terms of heat supply to DHN. The lowest heat supply is seen in Price-Limit with RCP8.5 climate condition using electricity price in 2022, which is decreased by 64.6% to only 7.94 GWh from 22.45 GWh of the baseline. It's been explained beforehand that the average electricity price in 2022 was the highest among other four years, meaning that the annual heat supply to DHN also is the lowest if one should consider Price-Limit which is very sensitive to electricity price. When the heat revenue can't offset the electricity cost to drive heat pump compressor, then there will be no heat injection to DHN with Price-Limit. An extreme situation where electricity could be higher than 2022 will

lead into much lower heat supply than the baseline. The following figure 26 displays the performance evaluation of different heat supply scenarios to DHN, giving more context on how the heat supply is distributed in accordance with different outdoor temperatures and changes in DHN supply temperatures.

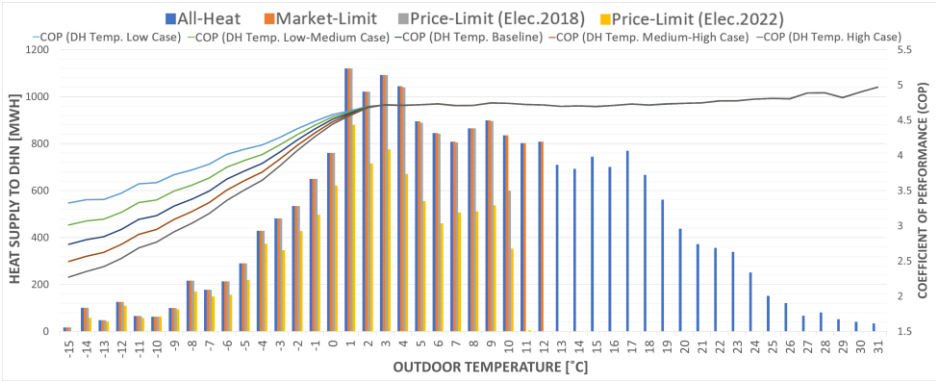

Figure 26. COP and Heat Supply to DHN according to Outdoor Temperatures

Figure 26 particularly demonstrates the heat supply distribution within different range of outdoor temperature plotted with Coefficient of Performance (COP) of operating the heat pump. It can be refined from figure 26 that for each range of outdoor temperature, the lowest heat supply occurs in Price-Limit using the highest electricity price (i.e., electricity in 2022). The amount of heat supply in Price-Limit using electricity price 2018 is still comparable with both All-Heat and Market-Limit until the outdoor temperature reaches 9ºC. It then starts becoming lower than All-Heat and Market-Limit when the outdoor temperature is at 10ºC, and further there's no heat supply with higher outdoor temperature. It's worth noting that figure 26 is plotted in the same TMY condition and in that case, the outdoor temperature of beyond 10 ºC represents 39.35% of total yearly hours (i.e., 3447 out of 8760 hours per year).

It's also interesting to see that most of the available heat is still generated at peak loads. It's not until the outdoor temperature starts to warm up, and particularly when the outdoor temperature reaches beyond 12 ºC, then there's no heat injection within Market-Limit scenario. At certain level of outdoor temperature (i.e., when the outdoor temperature in Stockholm reaches beyond 10ºC), it can be refined that it's not profitable for DC owner to inject the heat, if one should consider heat supply method using Price-Limit, which is inferred by zero heat supply in the distribution profile when the outdoor temperature is more than 10 ºC. With Price-Limit supply scenario, it can be underscored that 40.18% of available waste heat from DC is not profitable should it be injected to DHN in the case of low electricity price (i.e., electricity in 2018). In the case when the electricity price is high (i.e., electricity in 2022), the amount of waste heat not injected to DHN increases to 58.57%. On the other

hand, in the case of heat supply with Market-Limit, 31.87% of DC available waste heat can't be injected to DHN due to 12 ºC feed-in limit in the DHN. Figure 26 also informs us that the COP is sensitive to the change of DHN supply temperatures. Within low outdoor temperature (i.e., from -15 to 2ºC), the COP representing the lowest case of DHN supply temperature stands at the highest magnitude. It can be refined that the higher the case of DHN supply temperature, the lower the COP line of the heat pump for WHR. In the lower case of DHN, the DH supply temperature is also lower, which means the heat pump compression work is also lower. This lower compression work leads into higher COP, referring to equation 25 (i.e., lower $P_{HP.,comp}$ makes the COP higher). In the same correlation, the higher case of DHN causes the higher DH supply temperature which leads into higher heat pump compression work and ultimately lower COP. DHN supply temperature increases with the decrease in the specific low outdoor temperature which is in-line with figure 16 before, causing higher thermal supply. This increase in thermal supply level increases the temperature lift of the heat pump which causes the heat pump to do more compression work. COP is getting lower with more heat pump compression work, referring to equation 25 (i.e., higher $P_{HP.,comp}$ leads into lower COP). That explains why the COP line of high case being lower than the COP line of low case in specific low outdoor temperatures.

4.3 Technical KPIs

Previous chapter has demonstrated specific results on how cooling energy reduction is achieved in DC by means of WHR to DHN. Performance assessment is needed for each given configuration to measure techno-economic benefits that can be offered. The first part of performance assessment is geared towards primary technical KPIs which consist of PUE, ERF, and ERE. The secondary technical KPIs are denoted as $SPF_{thermal}$, SPF_{IT}, and HSPF. It's worthy to note that ERF, ERE, $SPF_{thermal}$, SPF_{IT}, and HSPF are not applicable to configurations A1 and A2 since both don't have WHR from server racks, meaning no heat injection value to DHN (i.e., $\dot{Q}_{DH}$ is zero). However, it's worthwhile to compare all four configurations in terms of PUE value. PUE metric informs us the total power consumption of the whole DC system compared to the power consumption of the IT Equipment only. PUE value stands more than 1 and is considered better with the lower value. The weekly PUE profile of each configuration within different seasons can be seen in the following figure 27.

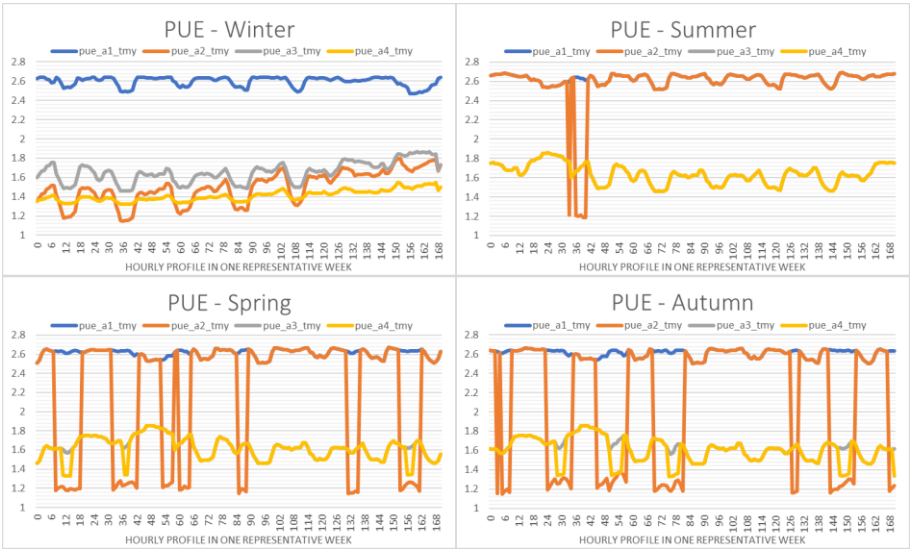

Figure 27. PUE Weekly Profile of Each Configuration within Different Seasons

PUE value in configuration A1 remains stable at 2.44 up to 2.68, regardless of the difference in outdoor temperature (i.e., comparing all four seasons). This happens because the cooling system in configuration A1 doesn't incorporate free cooling system which is highly dependent on outdoor temperature condition. It can be also seen that at some points, PUE in configuration A2 is measured lower than both configuration A3 and A4. This occurs because the total DC energy consumption of configuration A3 and A4 also includes heat pump compressor for WHR, leading into higher numerator in PUE fraction than configuration A2. The fluctuations occurring in spring and autumn demonstrates the dynamic influence of outdoor temperature to the DC total energy consumption in terms of cooling. There're times when the outdoor temperatures are low enough to enable free cooling which leads to cooling energy saving through the reduction of cooling consumption. On the other hand, PUE of configuration A4 is always either lower or the same with PUE of configuration A3. With the free cooling and waste heat recovery being applied in configuration A4, the cooling energy consumption in configuration A4 reaches its peak during summertime which has maximum value to configuration A3 level, as explained previously in sub-chapter 4.1. This condition leads into the same PUE value between configuration A3 and A4 in the summertime because the free cooling system is limited. The weekly PUE distribution profile as shown in figure 27 helps emphasize the correlation between each DC's power consumption in specific time, considering not only IT equipment, but also DC's cooling power and heat pump compressor power.

The highlighted information of PUE can be demonstrated by showing the summary of annual average PUE of all configurations as depicted in the figure 28.

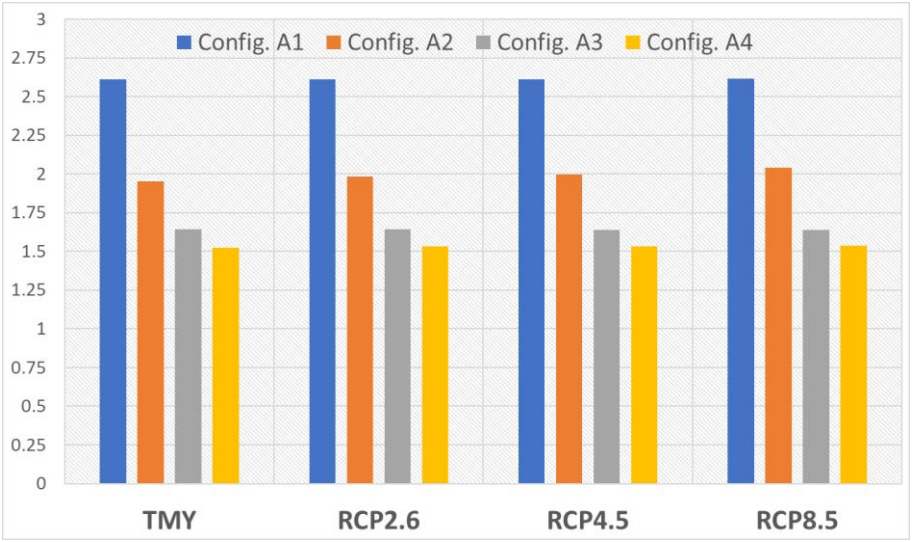

Figure 28. PUE Summary within Different Configurations and Climate Conditions

From figure 28, it can be refined that configuration A4 is the best performer with the lowest value of PUE. For example, in the same TMY condition, PUE of configuration A4 stands at 1.52, compared to 2.61, 1.95, and 1.64 for configurations A1, A2, and A3 respectively. On one specific hand, the tested variable for different climate conditions doesn't change the PUE value significantly. Despite the fact the total DC energy for configuration A3 and A4 also include the heat pump compressor because of WHR to DHN, it turns out the total energy consumptions of configurations A1 and A2 are still higher than configurations A3 and A4, which lead into higher PUE values. This can be explained as additional heat pump energy to recover waste heat can reduce DC's cooling energy more than it uses, by reducing energy consumed by chiller and CRAH cooling system. The cooling consumption which constitutes a significant portion of DC power consumption is getting lower from configuration A1 to configuration A4.

From the PUE value, one can obtain an understanding that configurations A3 and A4 perform better than configurations A1 and A2. However, since PUE metric doesn't consider heat supply to DHN, one needs to also obtain in-depth insights about waste heat recovery variable (i.e., energy reused to DHN). The following KPI denoted as ERF informs us how much heat that is supplied to DHN compared to the total energy in data centre. The summary of annual average ERF values of all scenarios can be found in the figure 29.

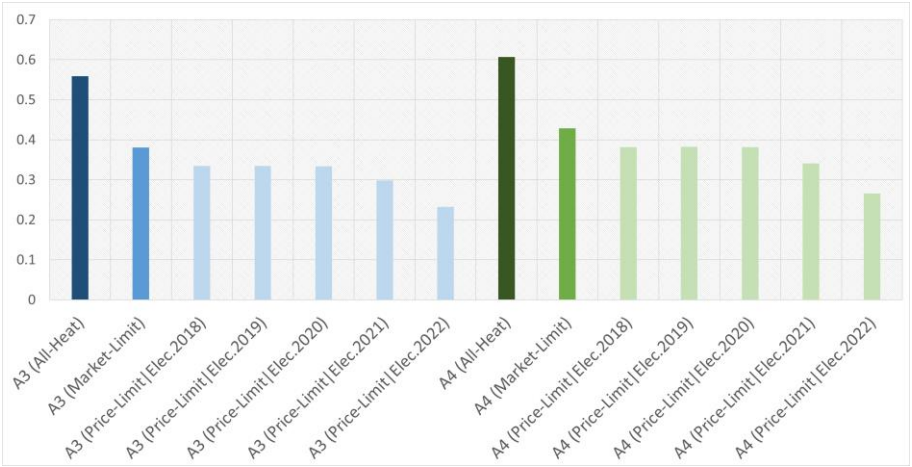

Figure 29. ERF Summary within Different Configurations and Electricity Prices

Higher ERF value is deemed better as it means the more DC's energy is reused [51]. In general, configuration A4 has higher ERF value than the A3 despite the fact the difference is not significant. For instance, within All-Heat, the ERF value of configuration A4 is 0.61 compared to 0.57 in configuration A3. The effect of climate change is not significant as already explained in previous sub-chapter 4.2. Despite that fact, there's still a contribution of the difference in outdoor temperature but not significant, hence not plotted in the figure. Due to that fact, it's worthwhile to note that the plotted ERF summary above is solely focused on the same climate condition (i.e., TMY). The ERF value of All-Heat scenario is higher than the ERF of heat Market-Limit and Price-Limit scenarios because higher heat supply will lead into higher value in the ERF numerator fraction. On the other hand, the influence of electricity price is again discovered to have more significance when comparing electricity price between 2018 and 2022 for instance. The electricity price with higher annual average will generate less amount of heat supplied to DHN, which also means the lower ERF. The best ERF performer goes to configuration A4 with All-Heat scenario, reaching the annual average ERF value of 0.61. The lowest ERF value of 0.26 is generated by configuration A3 should the heat be supplied with Price-Limit and applied with electricity price of 2022. It can be refined in other words that the higher electricity price will further result in the lower ERF.

The next KPI pertains to ERE which correlates the ERF and PUE metrics according to the equation 30 before. The annual average of ERE values within different configurations, climate conditions, and electricity prices can be summarized with the following figure 30.

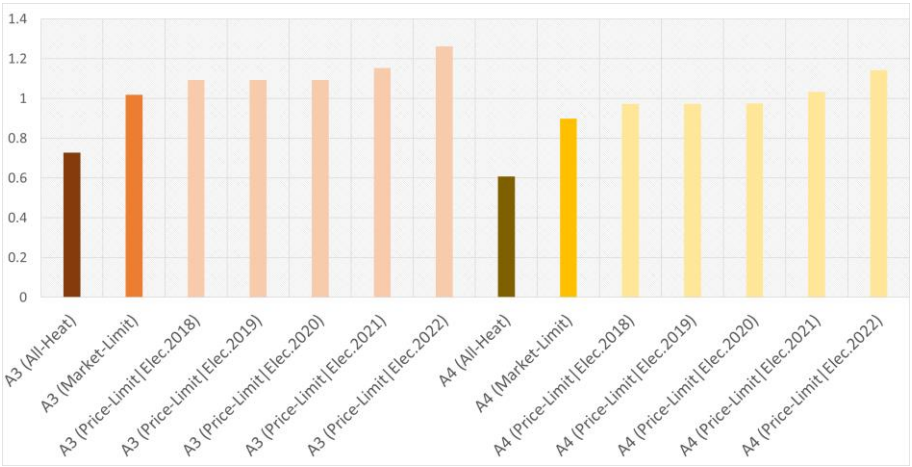

Figure 30. ERE Summary within Different Configurations and Electricity Prices

As it can be seen from figure 30, the ERE of configuration A4 with All-Heat supply is the best performer because of its lowest value, measured at 0.59. ERE with lower value is considered better. For ERE, the range is 0 to infinity and it allows values of less than 1.0 [51]. An ERE of 0 means that 100% of the DC's energy is reused. Comparing the different electricity price in the same climate condition, one can see the high influence of the electricity price on ERE value. The highest ERE value of 1.26 goes to configuration A3 with Price-Limit supply, using electricity in 2022. It can be refined that lower electricity price leads into lower ERE. For instance, from that previous ERE value of 1.26, the number will change into 1.09 if one should change the electricity price from 2022 to 2018 in the same climate condition and heat supply scenario. That electricity change is translated into 12.6% of difference in ERE value. The result informs us that the electricity price also plays roles in changing the KPI performance, in this case the ERE metric itself.

Even though the ERE value compliments ERF value in such way that they both result in the same configuration which has the best performance (i.e., configuration A4 using All-Heat scenario in TMY condition), but as stated by Oltmanns J. et al., the disadvantage of this approach is that different exergy level leads into the difference between the different energy forms in terms of their quality [52]. More proper and in-depth analysis regarding the energy reused is hereby proposed. In this way, it's emphasized that one should incorporate secondary technical KPIs; $SPF_{thermal}$, SPF_{IT}, and HSPF to understand how much the energy brought to DC is reused ($\dot{Q}_{DC}$) when compared to specific parameters; namely the DC's heat margin consumption, IT equipment, and the heat pump compression for DHN purpose. The denominator of $SPF_{thermal}$ fraction is called the heat margin which results from subtracting the total energy in DC ($\dot{E}_{DC}$) and the IT equipment ($\dot{E}_{IT}$), as explained in

previous sub-chapter 3.3.1. It's worthwhile noting that only the $SPF_{thermal}$ value can be applied to configurations A3 and A4 since it involves different cooling power consumptions between those two configurations. On the other hand, the SPF_{IT} and HSPF are the same for both configurations A3 and A4 (i.e., both the fractional numerator and denominator are the same due to the same IT and heat pump compression power). The values of $SPF_{thermal}$, SPF_{IT}, and HSPF are mathematically bounded from 0 to infinity. Figure 31 summarizes the annual average of HSPF, $SPF_{thermal}$, and SPF_{IT} within different configurations, climate conditions, and electricity prices.

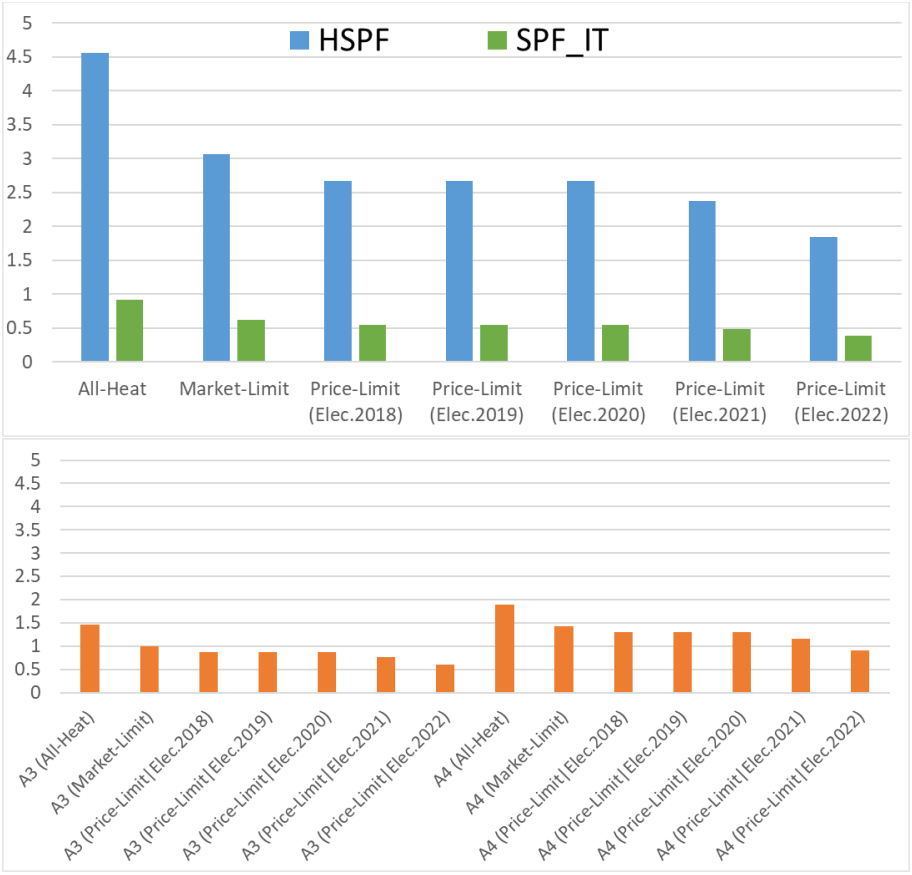

Figure 31. Summary of Secondary Technical KPIs: HSPF and SPF_{IT} (top); and $SPF_{thermal}$ (bottom)

From figure 31, All-Heat supply always generates the highest value for each SPF category. It can be also seen that in terms of magnitude, the HSPF metric stands at the highest, followed by $SPF_{thermal}$ and SPF_{IT} respectively. The effect of climate outdoor temperature is also neglected as per previous results in sub-chapter 4.2. While on the other hand, changing the electricity price

again influences each of SPF category in the way that the higher electricity price will lead into lower SPF value accordingly.

With $SPF_{thermal}$, one can compare the performance between configuration A3 and A4. The higher $SPF_{thermal}$ value of more than 1 means the energy that is reused is bigger than the marginal heat energy brought into DC's system. Configuration A4 has higher $SPF_{thermal}$ value than A3 in the same condition. For instance, with Price-Limit scenario using electricity price in 2018, the configuration of A4 reaches 1.31, compared to 0.86 in configuration A3. Again, with this metric, the best performer is awarded to configuration A4 with All-Heat scenario. It can be seen from its value which is measured at 1.89, being the highest value for $SPF_{thermal}$. The influence of higher electricity price (for instance, changing electricity price from 2018 to 2022) will lower its value because of lower heat supply to DHN as previously explained in subchapter 4.2. The lower heat supply to DHN means the lower energy reused in the DC (i.e., lower $\dot{Q}_{DH}$ as the numerator), leading to lower $SPF_{thermal}$ value. The lowest $SPF_{thermal}$ value belongs to configuration A3 with electricity price 2022 which stands only at 0.6.

From the given SPFs results, one can also understand how valuable the recovered waste heat compared to the energy consumption in DC. From HSPF standpoint, it can be informed that the reused energy can reach up to 4.5 times higher than the heat pump compression energy. From $SPF_{thermal}$ perspective, it can be understood that the reused energy can be worth 1.89 times higher than the marginal heat of data centre. However, from the SPF_{IT} perspective, the reused energy is lower than IT energy consumption, inferred by its value which is lower than 1 (i.e., 0.91 using All-Heat supply in TMY condition,). The IT equipment consumption is lower than the total DC energy but higher than for instance the heat pump power consumption, and hence, the HSPF value becomes higher than SPF_{IT} since the fractional denominator in HSPF is lower than SPF_{IT}. Recalling the previous result of ERF (i.e., for the same configuration A4 in TMY condition), the ERF value is also measured at 0.61 (i.e., lower than 1 as well). It can be translated in other words that the reused energy is worth 91% from the total IT equipment consumption and 61% from DC total energy consumption. In general understanding, those three SPFs compliment the previous KPIs, giving the clear result that configuration A4 with All-Heat supply in TMY condition is the best performer due to its highest value in each SPF category.

4.4 Economic KPIs

The result of economic KPI is presented by the calculation of lifecycle operational expense (i.e., Lifecycle OPEX or LCO) which has been formulated in the previous sub-chapter 3.3.2. The calculation of LCO for each configuration uses 3% discount rate. The operational lifetime for heat selling to DHN refers to an initial contract between Stockholm Exergi and heat supplier which typically runs for 10 years [57]. Figure 32 shows the LCO results for each configuration within different electricity prices.

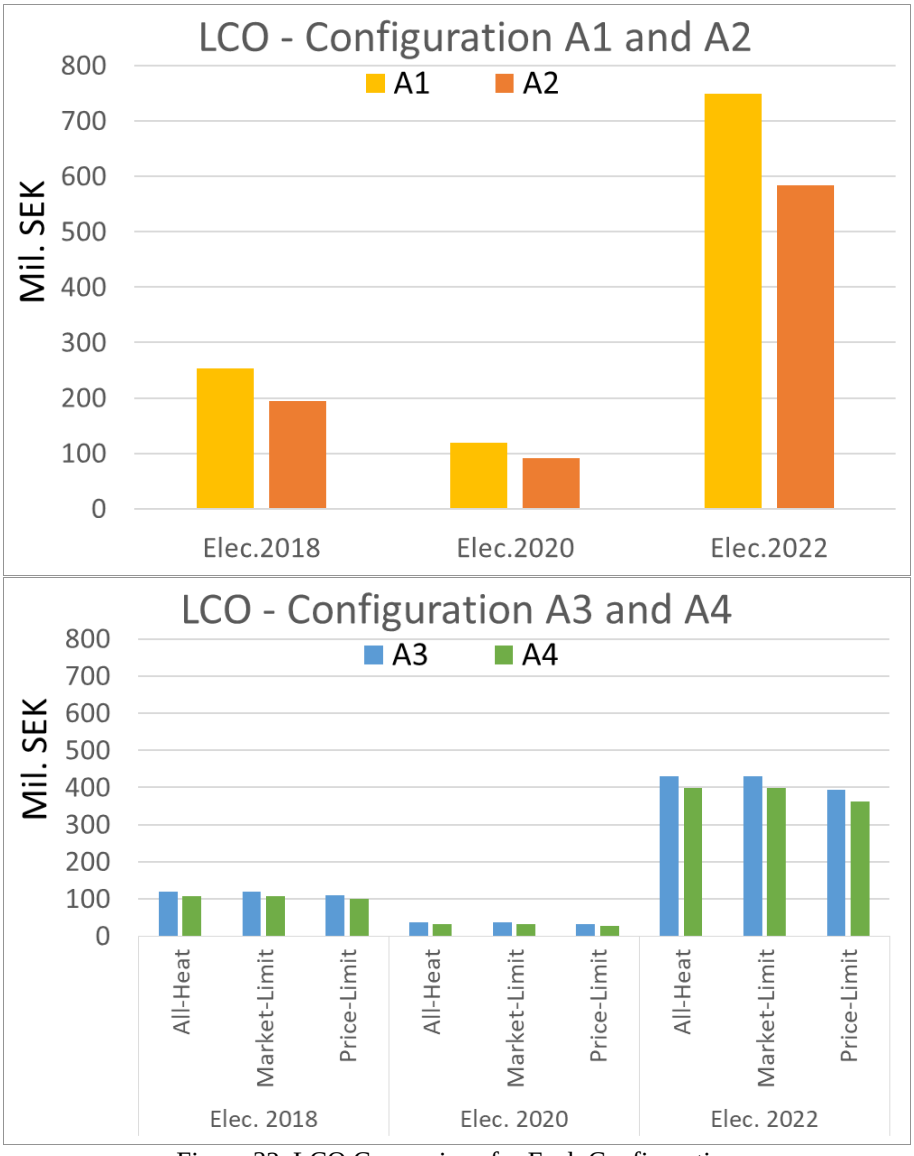

Figure 32. LCO Comparison for Each Configuration

From the figure 32, the LCO of configuration A1 using electricity price in 2022 is the highest among other configurations. The effect of climate change is neglected due to insignificant influence on the LCO, following the previous results. On the other hand, there's a significant influence in terms of using different electricity price, in such way that the higher electricity price will also lead into higher LCO. In that case, the highest electricity price (i.e., electricity in 2022) constitutes to the highest LCO and the lowest electricity price (i.e., electricity in 2020) to the lowest LCO.

From such monetary value perspective, running DC in BaU scheme (i.e., configuration A1) is not preferable due to its high LCO. For instance, LCO in configuration A1 is measured at 748 million SEK by using 2022 electricity data. Should DC owner convert their DC cooling system by using free cooling (i.e., moving from configuration A1 to A2), the LCO can be reduced to 583 million SEK, or in other words, a decrease in LCO by 22% in the same condition of climate and electricity price. Furthermore, if DC owner should consider both using free cooling and recovering their waste heat to DHN at the same time with Market-Limit scenario (i.e., moving from configuration A1 to A4 at Market-Limit heat supply scenario), the LCO can be decreased by 46.8% to 398 million SEK. It can also be refined that in terms of heat supply to DHN (i.e., applied to only configuration A3 and A4), the lowest LCO is seen within the Price-Limit supply. The reason of this can be explained as heat supply with Price-Limit scenario only supplies the heat when the revenue of heat supply to DHN is higher than the electricity absorbed by the heat pump to upgrade the waste heat. For instance, the LCO will become 363 million SEK by using Price-Limit scenario compared to previously 398 million SEK of using Market-Limit scenario within the same configuration A4. On the other hand, heat supply with All-Heat scenario injects all available waste heat without considering the cost to run the heat pump while heat supply with Market-Limit just covers the cost of electricity for the heat pump when selling the low amount of heat during summertime.

The parameter of LCO provides useful information regarding the maximum capital expenditure (CAPEX) that one can consider when the investment of WHR for DHN is made. Figure 33 demonstrates a sensitivity analysis of the discount rate for the calculated LCO within different configurations.

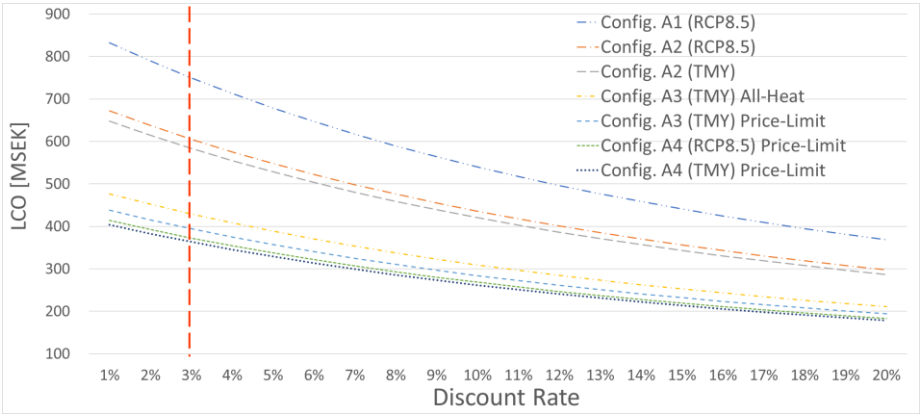

Figure 33. Discount Rate Sensitivity Analysis

It's worthwhile to note that figure 33 is plotted in accordance with electricity price in 2022 which also represents the latest electricity data of the time that this thesis is written. 3% is the nominal rate used in the LCO analysis as the chosen lower benchmark and marked with a red bar. The sensitivity analysis of having different discount rate is plotted to give multiple benchmarks if one should consider different discount rate to accept the maximum CAPEX when transitioning to specific configuration. For example, assuming the discount rate of 3% and electricity price of 2022 in RCP8.5, if DC owner should consider moving from configuration A1 to A4 with Price-Limit supply, the difference in LCO between those two configurations will be 377 million SEK, which can be also deemed as the maximum CAPEX that can be afforded by the DC owner for the calculated 10 years lifetime. The higher discount rates will lead into lower LCO and favour lower CAPEX with more costs deferred to the future. For instance, using 15% rate in the same conditions from previous explanation (i.e., configuration A1 to A4 with Price-Limit supply in RCP8.5), the maximum CAPEX will decrease by 41.16% to 222 million SEK.

On the other hand, it's deemed more important to give broader context in the case of Stockholm which is situated in the cold climate region (i.e., compatible for using free cooling as represented by configuration A2). Hence, the summary of maximum CAPEX to transition from configuration A2 to both configuration A3 and A4 can be summarized in the following figure 34.

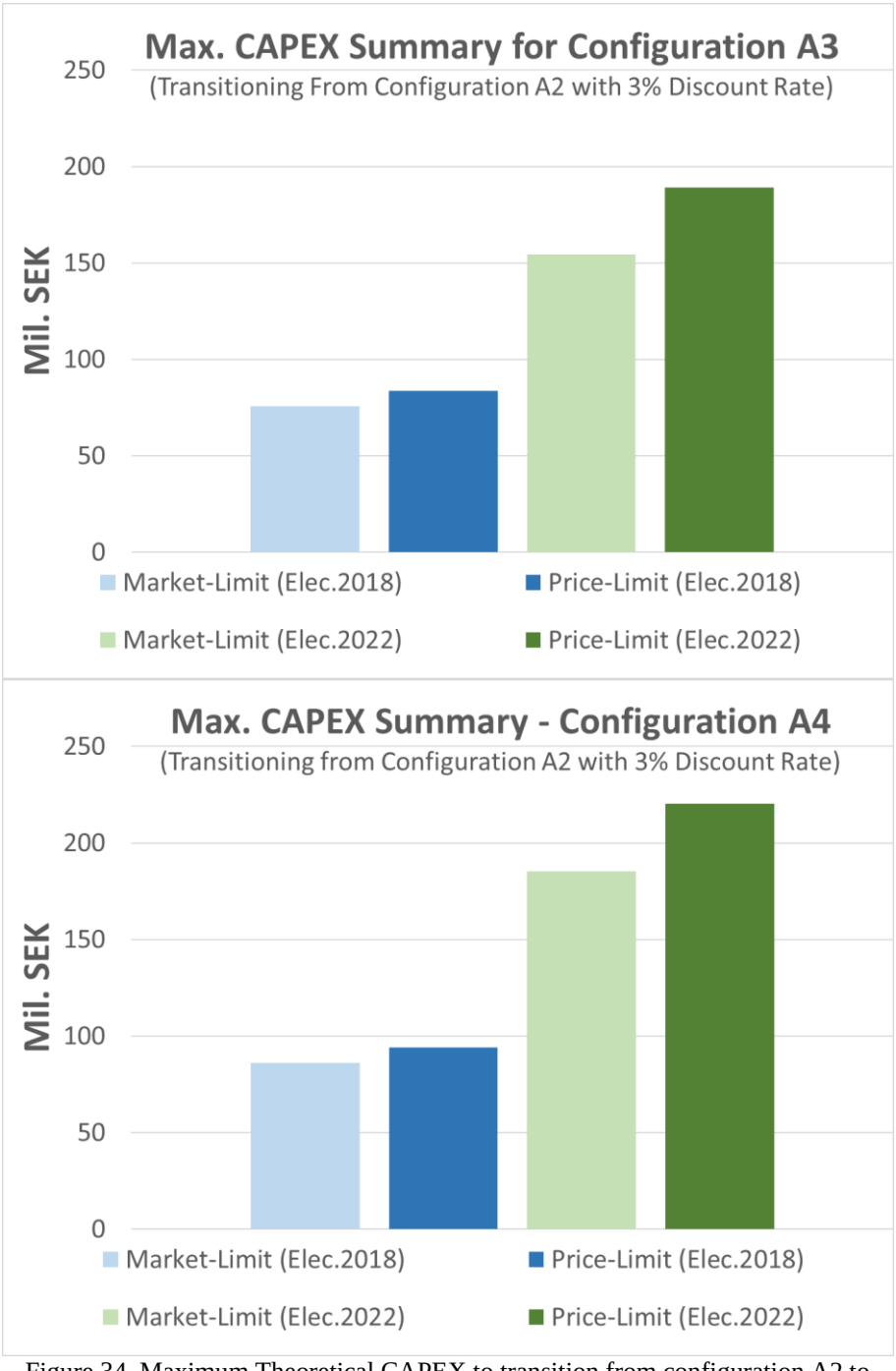

Figure 34. Maximum Theoretical CAPEX to transition from configuration A2 to configuration A3 and A4

It can be seen from figure 34 that the maximum CAPEX for configuration A4 is higher than configuration A3. This can be explained as the LCO in configuration A4 is lower than configuration A3 as already mentioned in the result of previous figure 32. It can be also refined that maximum CAPEX with Price-Limit supply is also higher than Market-Limit supply in the same year of electricity price being used. The lower the LCO, the higher the potential saving in the system configuration which leads into higher amount of maximum CAPEX that one can consider. It can be seen from figure 34 that, should the electricity in 2018 be adapted, the maximum CAPEX for DC owner to transition from configuration A2 to configuration A4 is 86 million SEK within Market-Limit supply condition. The Market-Limit supply represents the current ODH business-model in Stockholm as previously explained in sub-chapter 3.4. On the other hand, should the case of electricity in 2022 be used, the maximum CAPEX will increase by 15.11% to 185 million SEK (i.e., from previously 86 million SEK in the same heat supply with Market-Limit).

The LCO results produce different economic outcomes in terms of possibilities. The LCO will increase if the electricity prices remain high, for instance when the electricity price stands at 2022 level compared to 2018 or 2019. On the other hand, the climate outdoor is still a less critical variable. According to figure 32, the best performer of economic KPI belongs to lowest LCO which is awarded to configuration A4 with Price-Limit supply by using electricity price 2020, and this is only specific choice of condition with given environmental conditions that a DC is responding to. Recalling the results from previous technical KPIs, the best performer eventually goes to configuration A4 with All-Heat supply within the same electricity price. In other words, there's a difference in awarding which heat supply scenario is the best performer, in terms of technical and economic KPIs. Despite that fact, to such extent, all KPIs agree that configuration A4 is the best performer with both lowest electricity price (i.e., electricity in 2020), and lowest climate outdoor temperature (i.e., TMY condition). In that case, one needs to be provided with additional context on how new insights from different perspective can be obtained when comparing All-Heat and Price-Limit scenarios. Figure 35 provides sensitivity analysis to help understand if different DHN supply temperatures are applied, then how it affects both the LCO of Price-Limit and All-Heat supply scenarios.

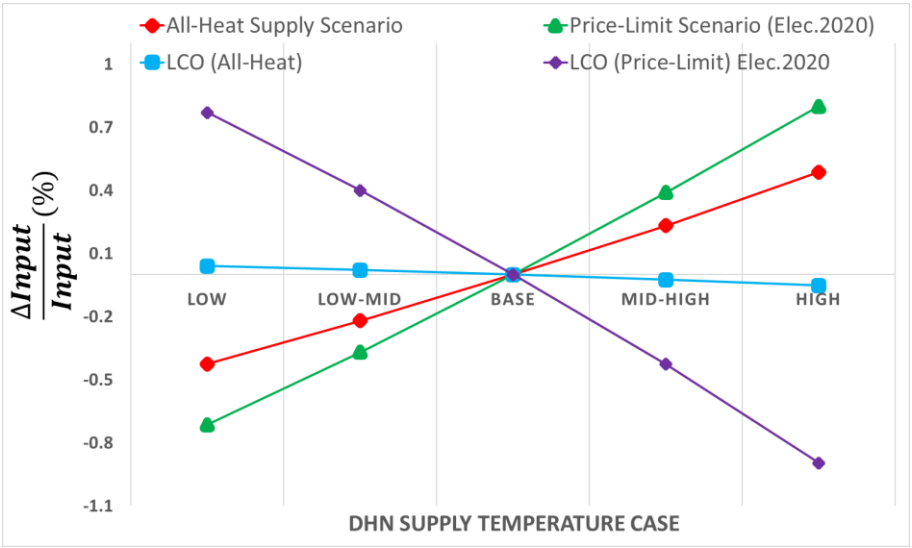

Figure 35. Sensitivity Analysis of DHN Supply Temperature to Heat Supply Scenario and LCO using Electricity Price in 2020

The DHN supply temperature is varied into five different cases according to previous explanation in sub-chapter 3.4. From the sensitivity result in figure 35, it can be seen that when the DHN supply temperature is made higher from the baseline, there's an increase in the amount of heat supplied for both All-Heat and Price-Limit scenarios, but the difference is small. For instance, the change of heat supply with Price-Limit and All-Heat from the baseline to the high case of DHN supply temperature is only 0.8% and 0.48% respectively. With this small percentage, it can be refined in other words that heat supply in DC is very insensitive to DH network temperatures. DC that supplies more heat with higher DHN supply temperature is compensated by lower COP as previously explained in the figure 26. It's been demonstrated that lower COP of WHR heat pump is related to the higher case of DHN supply temperature. On the other hand, when the supply temperature in the network is decreased, the amount of DC waste heat that can be injected to DHN will also be decreased, resulting in lower heat supply for both scenarios, but again this number is insignificant (i.e., -0.71% and -0.42% for Price-Limit and All-Heat supply scenarios respectively). The results inform us that heat supply with Price-Limit is more sensitive to the change in DHN supply temperature than All-Heat scenario; but from the magnitude perspective, it's not significant. The same thing also applies in the context of heat supply in DC which is also not too sensitive to the change of DH network temperatures.

On the other hand, with higher supply temperature, the LCO for both All-Heat and Price-Limit scenarios decrease because of the higher heat revenue that can be harnessed from selling more heat in higher DHN supply temperature. This

higher revenue through heat selling reduces the operational cost, leading to lower LCO as well. It's also interesting to see that how vulnerable Price-Limit supply is to the change in supply temperature compared to All-Heat supply. The sensitivity in high case shows that there's a decrease in LCO by -0.9% for Price-Limit supply compared to -0.05% for All-Heat supply. And again, this informs us that there is a very limited relationship between the change in DHN supply temperature and the LCO. With the heat pump being less efficient due to the increase in the heat injection and when the DC can filter the profitable hours, it also means that it can generate more profits on the profitable hours. On the other hand, one can also recall the previous figures 22 in which the amount of heat supplied with Price-Limit is lower than All-Heat. Even though the change in heat supply for Price-Limit is greater than All-Heat scenario, but the heat accumulation with Price-Limit will always be lower than All-Heat supply as the baseline (i.e., All-Heat is the maximum waste heat available from DC that can be reused).

5. Discussion

In the results of chapter 4.1, it's well noted that configuration A1 is the least efficient compared to the other configurations. Being the largest power consumer in DC, the cooling system in configuration A1 results in 55.8% of total energy consumption. Data centre shouldn't consider running the business in BaU scheme (i.e., configuration A1) compared to other configurations. The annual cooling energy from the baseline can be decreased by 75.1% (i.e., from 35.73 GWh to 8.89 GWh) in configuration A4 by doing both waste heat recovery and free cooling. If the benchmark is made to configuration A2 (i.e., using free cooling), the associated cooling energy can be reduced by 55.61% (i.e., from 20.04 GWh to 8.89 GWh) in configuration A4. With configuration A4, waste heat is reused, and the free cooling (FC) saves the energy consumption by taking advantage of cold outdoor air to replace the cooling energy that would otherwise require CRAH to produce the chilled water to cool down the supply air.

In the results of chapter 4.2, the converted cooling energy into waste heat recovery for DHN purpose has been developed into three different heat supply scenarios. The annual heat supplies in this thesis work are measured at 22.45, 15.31, and 13.44 GWh for All-Heat, Market-Limit, and Price-Limit scenarios respectively which represent 3.15 MW of IT power rating used in this thesis work. The amount of heat supply to DHN will always differ from one case to another, depending on the contract between the DHN operator and the DC owners. For example, Yandex DC in Mäntsälä, Finland with IT capacity of 10 MW is reported to have annual recovered waste heat of around 20 GWh [58]. Tieto DC is Espoo, Finland with 2 MW of IT capacity has the amount of recovered waste heat estimated at 30 GWh per annum [58]. It can be said in other words that there's no such general rule on how much waste heat can be injected to DHN per MW of IT capacity. This thesis work has provided multiple scenarios and conditions to support the decision making by doing techno-economic analysis of recoverable waste heat from DC. The final heat supply that the DHN can purchase from DC owner is dependent on the unique business case.

In this study, each heat supply scenario to DHN is examined with different electricity prices and outdoor temperatures. The main result has been highlighted, in which the electricity price has more significant impacts than the outdoor temperature to influence the amount of heat supplied. From the result of performance evaluation of heat supply as the function of outdoor temperature, it has been underscored that at certain level of outdoor temperature (i.e., when the outdoor temperature in Stockholm reaches beyond 10ºC), it's not profitable for DC to inject the heat, if one should consider heat supply method

using Price-Limit in that condition. From the result, it's also observed that COP of heat pump increases with the rising outdoor temperature, ranging from 2.27 to 4.96 for the plotted outdoor temperature from -15ºC to 31ºC. The overall increase in COP to the overall increase in outdoor temperature is also seen in the heat pump model conducted by Jeter S.M. et al. [55].

In chapter 4.3, the results of six different technical KPIs have also been analysed for each applicable configurations within different conditions. An inefficient DC's energy system according to Research Institutes of Sweden (RISE) results in PUE value of 1.8 until 2.5 or higher [54]. Moving from configuration A2 to A4 in this case brings PUE value from 1.95 to 1.52, which means significant reduction of DC energy consumption is achieved in configuration A4. On the other hand, the further result also confirms that configuration A4 with heat supply All-Heat has the highest ERF value, reaching 0.61 in TMY condition. ERF value of above 50% is also seen in the WHR case study of one of data centres in Barcelona, Spain conducted by E. Oró et al. [24]. The ERF result clearly informs that more than half of DC energy consumption can be reused for heat supply to DHN (i.e., ERF 0.61). On the same hand, the confirmation of that ERF result is also in-line with ERE which also states that configuration A4 with All-Heat supply in TMY condition as the best performer, with ERE value measured at 0.59. It can also be refined from the results that the influence of outdoor temperature is less significant than the electricity price for both ERF and ERE. Unlike ERF which always considers the highest value, the ERE in contrast considers the lowest value as the best performer.

However, the disadvantage of this ERE approach is the difference in exergy level as mentioned by Oltmanns J. et al. [52]. The thesis has suggested three additional performance metrics as secondary KPIs to replace ERE. The parametrical evaluation of ERE is similar with PUE, looking for lowest values for both. Furthermore, both ERE and PUE have the same fractional denominator, that is the IT energy consumption. Moreover, the highlighted results of PUE, ERF, and ERE are the same, confirming configuration A4 as the best performer. To avoid the exergy complexity in ERE, the thesis has revisited that it's sufficient to emphasize PUE and ERF as the primary technical KPIs which just need to be further analysed with secondary technical KPIs, namely $SPF_{thermal}$, SPF_{IT}, and HSPF. Those KPIs are reliable when tested with different outdoor temperatures and electricity prices. The same observation is seen in the way that electricity price has greater influence than the outdoor temperature for the given KPIs. The higher both climate outdoor temperature and electricity price, the worse the SPFs metrics accordingly. In addition to that, secondary technical KPIs have complimented primary technical KPIs, giving the same results that configuration A4 with All-Heat supply in TMY condition is the best performer due to its highest value in each SPF category.

It's also interesting to see that according to economic KPI (i.e., using LCO), the best performer goes to the lowest LCO which is configuration A4 with Price-Limit supply using electricity price of 2020. While on the other hand, the best performer according to technical KPIs belongs to configuration A4 with All-Heat supply. Despite that fact, both technical and economic KPIs agree that configuration A4 in TMY condition should be considered by DC owner as the chosen system configuration. Price-Limit supply (i.e., inject the heat when the heat selling revenue is positive) is deemed more favourable in terms of better LCO than in All-Heat supply. This can be explained as the heat supply in All-Heat is not dependent on the electricity price. Heat supply in Price-Limit reduces the operational cost by only operating heat pump when the heat selling to DHN can offset the price of electricity. With the lowest electricity price used (i.e., electricity in 2020), one can see a significant reduction in LCO compared to both All-Heat and even Price-Limit using higher electricity price (e.g., electricity in 2022). On the other hand, All-Heat scenario injects all available waste heat to DHN regardless of the profitability of selling the heat itself (i.e., no consideration of electricity cost to operate the heat pump). Different conclusion between technical and economic results is commonly seen in the research studies. For example, even though the metrics of the primary energy reused can be above 50%, it turns out that the economic analysis performed for a specific 1 MW data centre located in Barcelona (Spain) demonstrates the non-viability of heat recovery integration in most of the conventional air-cooled data centres [24]. In that case, they considered capital expenditure (CAPEX) and operational expenditures of heat recovery solutions [24]. The results in this thesis work may vary since it doesn't consider full investment analysis. However, the specific result of maximum theoretical CAPEX has been presented as of figure 34. The result has provided a theoretical amount of maximum capital investment that DC owners can pursue, should they transition from configuration A2 to configuration A3 and A4. It's worthwhile to note that the result is specifically applied to the case of Stockholm ODH in Sweden. Different electricity prices, climate conditions, applicable DHN cases within different regions may lead into different results.

It can also be refined from the results that the difference between technical and economic conclusion is only addressed to the heat supply scenario standpoint. The sensitivity analysis has been conducted to provide more insights on how the heat supply scenario will affect the LCO as the economic parameter in accordance with the change in DHN supply temperature. Even though the amount of heat supplied by Price-Limit is lower than All-Heat scenario, but the sensitivity indicates that the LCO in Price-Limit can be made lower with higher supply temperature in DHN. All-Heat supply is less sensitive to the change in supply temperature than Price-Limit supply since it's not dependent on the change in electricity price to operate the heat pump in meeting the higher heating demand.

6. Conclusions

This thesis project has demonstrated technical and economic analysis of Data Centre (DC) being prosumer in district energy systems in Stockholm region. The maximum recommended capital expenditure (CAPEX) for DC's owner in Stockholm to transition from "free-cooling only" to both using "waste heat recovery and free-cooling" configuration is 86 million SEK for the case should electricity in 2018 be adapted. In the case when higher electricity price (i.e., electricity in 2022) is applied, the maximum recommended CAPEX will be 185 million SEK. The results obtained in this thesis project have given new insights to DC owners on why they should consider recovering DC's waste heat to District Heating Network (DHN) for the case of Stockholm region.

The research questions particularly ask these followings:

1. In which system configuration will the DC energy system produce the most favourable performance?
2. What techno-economic benefits will the configuration(s) have when compared to stand-alone DC without waste heat recovery?
3. How do outdoor temperature and electricity price influence the performance of each system configuration?

To the first question, a DC with free cooling and waste heat recovery is the best system configuration that DC owners should choose when deciding to transition their DC energy system into more energy efficient. Both the free cooling and waste heat recovery contribute to better energy performance in DC by saving cooling energy and reusing energy that would otherwise be wasted (i.e., upgrading the waste heat to DHN).

To the second question, the techno-economic benefits can be refined from the conclusions obtained in both technical and economic performance. Configuration with free cooling and waste heat recovery has shown that it can reduce energy consumption by 55.6% from the DC using free-cooling system only by recovering the cooling waste heat and using free cooling in DC system. Power Usage Effectiveness (PUE) is also decreased from 1.95 to 1.52 and the Energy Reused Factor (ERF) value indicates that the reused energy can reach 61% from DC total energy consumption. Furthermore, the lowest Levelized Operational Expenditures (LCO) is accomplished with both free cooling and waste heat recovery when the DC is able to avoid heat injection during unprofitable hours of high electricity prices (Price-Limit supply scenario). The results further indicate that injecting all the heat (i.e., All-Heat supply scenario) is better from a technical standpoint, but limiting injection to specific hours (i.e., Price-Limit) is economically beneficial. On the other hand, both heat supply and LCO are concluded to be not sensitive to the change of DH

network temperatures. Price-Limit supply is more sensitive with the change in supply temperature compared to All-Heat; but from the magnitude perspective, both are not significant.

To the third question, results show that the electricity price has more significant impacts to both the heat supply and the overall KPIs than the influence of climate change. The presence of rising outdoor temperatures through higher climate conditions is existed but it's not significant. The higher outdoor temperature will lead into lower heat supply since the DHN supply temperature declines with the rising outdoor temperature. On the other hand, in the case of low electricity price, 40.18% of the annual available waste heat in DC is not profitable should it be injected to DHN. In the case if the electricity price is higher, the number goes up to 58.57%. The higher the electricity price, the lower the amount of waste heat that can be injected to DHN within Price-Limit supply because it's more expensive to operate the heat pump than selling the heat itself. With the lower heat supplied to DHN, the ERF will also become lower, resulting into the lower reused energy in DC system. The secondary technical KPIs (i.e., $SPF_{thermal}$, SPF_{IT}, and HSPF) will also decrease accordingly because of the lower heat supply. The higher electricity price has also greater impact to the LCO for each system configuration. The lowest LCO is seen in the configuration of using both waste heat recovery and free cooling, while the highest LCO is observed in DC's configuration running in Business-As-Usual (BaU) case (i.e., with neither waste heat recovery nor free cooling). Another conclusion obtained is that when the outdoor temperature in Stockholm goes above 10 ºC, it's not profitable for DC owner to inject the heat, if one should consider heat supply method using Price-Limit scenario. This is because the heat price is getting lower with the outdoor temperature being higher. When the revenue from selling the heat is small during certain outdoor temperature and it can't offset the electricity cost to drive heat pump compressor, then there will be no heat injection to DHN with Price-Limit scenario. In that case, it happens when the outdoor temperature goes beyond 10 ºC.

The thesis project has particularly proposed secondary technical KPIs to support the primary KPIs. It can be refined from the results that the conclusions in secondary KPIs are in-line with the primary KPIs, and so it can be used for the decision-making process, for the context of Data Centre operating as Prosumers in DHN. Future research may also be emphasized specifically on the techno-economic analysis of waste heat recovery from liquid-cooled DC technology using the newly proposed KPIs described in this project.

7. References

[1] IPCC, 2022, Summary for Policymakers. In Global Warming of 1.5°C: IPCC Special Report on Impacts of Global Warming of 1.5°C above Pre-industrial Levels in Context of Strengthening Response to Climate Change, Sustainable Development, and Efforts to Eradicate Poverty (pp. 1-24). Cambridge: Cambridge University Press. doi:10.1017/9781009157940.001.

[2] Tilia/TU Wien/IREES/Öko-Institut/FraunhoferISI, October 2021, Overview of District Heating and Cooling Markets and Regulatory Frameworks under the Revised Renewable Energy Directive: Main Report.

[3] International Energy Agency (IEA), District Heating, https://www.iea.org/reports/district-heating.

[4] Energiforsk, September 2020, Toolbox for Prosumtion in District Heating, Report 2020:696, ISBN 978-91-7673-696-8.

[5] Stockholm Exergi, Open District Heating (A Part of Stockholm Exergi): https://www.opendistrictheating.com/our-offering/ (Accessed: 2023-03-04).

[6] Chang Su, Dalgren J., Palm B., High-resolution mapping of the clean heat sources for district heating in Stockholm City, Energy Conversion and Management 235 (2021): 113983.

[7] CloudScene. Market profile Sweden. n.d. URL:https://cloudscene.com/market/data-centers-in-sweden/all (Accessed: 2023-03-04).

[8] International Energy Agency (IEA), Data Centres and Data Transmission Networks, https://www.iea.org/reports/data-centres-and-data-transmission-networks.

[9] Lygnerud K (Editor), Nielsen S, Persson U, Wynn H, Wheatcroft E, AntolinGutierrez J, Leonte D, Rosebrock O, Ochsner K, Keim C, Perez-Granados P, Ro-manchenko D, Langer S, Ljung M. Handbook for increased recovery of urban excess heat, 2022, ReUseHeat Project, Grant Agreement 767429, European Commission. Available at: https://www.reuseheat.eu/wp-content/uploads/2022/09/ReUseHeat-Handbook-For-Increased-Recovery-of-Urban-Excess-Heat.pdf (Retrieved 2023-02-02).

[10] Kazi Main Uddin Ahmed, Manuel Alvarez, Math H.J. Bollen, Reliability Analysis of Internal Power Supply Architecture of Data Centers in Terms of Power Losses, Electric Power Systems Research, Volume 193, 2021, 107025, ISSN 0378-7796, https://doi.org/10.1016/j.epsr.2021.107025.

[11] Ashrae T. Thermal guidelines for data processing environments–expanded data center classes and usage guidance. Whitepaper prepared by ASHRAE technical committee (TC). 2011;9.

[12] Rasmussen N. Guidelines for specification of data center power density [White paper No. 120] In: APC, editor; 2005.

[13] Ebrahimi K. et al., A review of data center cooling technology, operating conditions and the corresponding low-grade waste heat recovery opportunities, Renewable and Sustainable Energy Reviews, Volume 31, 2014, Pages 622-638, ISSN 1364-0321, https://doi.org/10.1016/j.rser.2013.12.007.

[14] Patel CD, A Vision of energy aware computing from chips to data centers. In:Proceedings of ISMME 2003. Tsuchiura, Japan; Dec1–3, 2003.

[15] P. Huang et al., A review of data centers as prosumers in district energy systems: Renewable energy integration and waste heat reuse for district heating, Applied Energy, Volume 258, 2020, 114109, ISSN 0306-2619, https://doi.org/10.1016/j.apenergy.2019.114109.

[16] Capozzoli A, Primiceri GJEP. Cooling systems in data centers: state of art and emerging technologies. 2015;83:484–93.

[17] International Energy Agency (IEA), Future of Heat Pumps, 2022.

[18] Cube, Steimle, F., Goodall, E. G. A., & Heinrich, I. M. (1981). Heat pump technology (Goodall, Ed.; Heinrich, Trans.). Butterworths.

[19] W. Grassi, Heat Pumps, Green Energy and Technology, DOI 10.1007/978-3-319-62199-9_2, Springer International Publishing AG 2018.

[20] Y.H. Venus Lun, S.L. Dennis Tung, Heat Pumps for Sustainable Heating and Cooling, Green Energy and Technology, https://doi.org/10.1007/978-3-030-31387-6, Springer Nature Switzerland AG 2020.

[21] B.S. Sadjjadi, et al., Energy flexible heat pumps in industrial energy systems: A review, Energy Reports, Volume 9, Supplement 3, 2023, Pages 386-394, ISSN 2352-4847, https://doi.org/10.1016/j.egyr.2022.12.110.

[22] R. Rahmani et al., A Complete Model for Modular Simulation of Data Centre Power Load, Journal of IEEE Transactions on Automation Science and Engineering, Vol. 14, No.8, August 2017

[23] M. Wahlroos et al., Utilizing data center waste heat in district heating – Impacts on energy efficiency and prospects for low-temperature district heating networks, Energy, Volume 140, Part 1, 2017, Pages 1228-1238, ISSN 0360-5442, https://doi.org/10.1016/j.energy.2017.08.078.

[24] E. Oró et al., Waste heat recovery from urban air cooled data centres to increase energy efficiency of district heating networks, Sustainable Cities and Society, Volume 45, 2019, Pages 522-542, ISSN 2210-6707, https://doi.org/10.1016/j.scs.2018.12.012.

[25] J. Yu et al., A simulation study on heat recovery of data center: A case study in Harbin, China, Renewable Energy, Volume 130, 2019, Pages 154-173, ISSN 0960-1481, https://doi.org/10.1016/j.renene.2018.06.067.

[26] Fabio G. et al., Techno-economic analysis of heat recovery from supermarket's CO2 refrigeration systems to district heating networks, Applied Thermal Engineering, Volume 193, 2021, 117000, ISSN 1359-4311, https://doi.org/10.1016/j.applthermaleng.2021.117000.

[27] Ham S.W., Kim M.H., Choi B.N., Jeong J.W., Simplified server model to simulate data centre cooling energy consumption, Energy and Buildings 86 (2015) 328 – 339, http://dx.doi.org/10.1016/j.enbuild.2014.10.058.

[28] TRNSYS 18 Mathematical Reference, a TRaNsient SYstem Simulation program (volume 4), 2019, Solar Energy Laboratory, University of Wisconsin-Madison and Thermal Energy System Specialists, LLC.

[29] CoolProp, Ian H. Bell, Jorrit Wronski, Sylvain Quoilin, and Vincent Lemort, Pure and Pseudo-pure Fluid Thermophysical Property Evaluation and the Open-Source Thermophysical Property Library CoolProp, Industrial & Engineering Chemistry Research 2014 53 (6), 2498-2508, DOI: 10.1021/ie4033999.

[30] An Investment Analysis, M.Pärssinen et al., Waste heat from data centers: An investment analysis, Sustainable Cities and Society, Volume 44, 2019, Pages 428-444, ISSN 2210-6707, https://doi.org/10.1016/j.scs.2018.10.023.

[31] Afonso, C., & Moreira, J. (2017), Data center: Energetic and economic analysis of a more efficient refrigeration system with free cooling and the avoided CO2 emissions, International Journal of Engineering Research and Application, 7(11 (Part-1)).

[32] Geng, Hwaiyu. Data Center Handbook, John Wiley & Sons, Incorporated, 2014. ProQuest Ebook Central, https://ebookcentral.proquest.com/lib/uu/detail.action?docID=1882156.

[33] Henchoz, S., Weber, C., Maréchal, F., & Favrat, D. (2015). Performance and profitability perspectives of a CO2 based district energy network in Geneva's City Centre. Energy, 85, 221–235. https://doi.org/10.1016/j.energy.2015.03.079.

[34] A. Carbó et al. Experimental and numerical analysis for potential heat reuse in liquid cooled data centres. Energy Conversion and Management, Volume 112, 2016, Pages 135-145, ISSN 0196-8904, https://doi.org/10.1016/j.enconman.2016.01.003.

[35] G.F. Davies, G.G. Maidment, R.M. Tozer, Using data centres for combined heating and cooling: An investigation for London, Applied Thermal Engineering 94 (2016) 296–304, http://dx.doi.org/10.1016/j.applthermaleng.2015.09.111.

[36] Norpool group, https://www.nordpoolgroup.com/en/

[37] Meteotest, Meteonorm Software V7, 2016, www.meteonorm.com.

[38] Park S. et al., J. Analysis of Air-Side Economizers in Terms of Cooling-Energy Performance in a Data Center Considering Exhaust Air Recirculation. Energies 2018, 11, 444. https://doi.org/10.3390/en11020444.

[39] Patterson MK, Tschudi W, VanGeet O, Azevedo D. Towards the net-zero data center: development and application of an energy reuse metric. ASHRAE Trans 2011;117:10–7.

[40] Mikko W. et al., Future views on waste heat utilization – Case of data centers in Northern Europe, Renewable and Sustainable Energy Reviews, Volume 82, Part 2, 2018, Pages 1749-1764, ISSN 1364-0321, https://doi.org/1.1016/j.rser.2017.10.058.

[41] Zimmermann S, Meijer I, Tiwari MK, Paredes S, Michel B, Poulikakos D. Aquasar: a hot water cooled data center with direct energy reuse, 2nd Int. Meet. Clean. Combust. CM0901-Detail. Chem Models Clean Combust Jul. 2012;43(1):237e45.

[42] S. Pelley, D. Meisner, T. F. Wenisch, and J. W. VanGilder, "Understanding and abstracting total data center power," in Workshop on Energy- Efficient Design, 2009.

[43] S.Sampath, Thermal Analysis of High End Servers Based on Development of Detail Model and Experiments, The University of Texas at Arlington, Arlington, 2012 (Master's thesis).

[44] World Bank, Climate Change Knowledge Portal For Development Practitioners and Policy Makers, https://climateknowledgeportal.worldbank.org/overview.

[45] D.Shin, S.W. Chung, E.Y. Chung, N. Chang, Energy-optimal dynamic thermal management: computation and cooling power co-optimization, IEEE Transactions on Industrial Informatics 6 (3) (2010) 340-351.

[46] C. Mateu-Royo, S. Sawalha, A. Mota-Babiloni, J. Navarro-Esbrí, High temperature heat pump integration into district heating network, Energy Convers. Manag. 210 (2020), 112719, https://doi.org/10.1016/j.enconman.2020.112719.

[47] Mahdi D. et al., Thermoeconomic and environmental feasibility of waste heat recovery of a data center using air source heat pump, Journal of Cleaner Production, Volume 219, 2019, Pages 117-126, ISSN 0959-6526, https://doi.org/10.1016/j.jclepro.2019.02.061.

[48] Krishna Kant, Data center evolution: A tutorial on state of the art, issues, and challenges, Computer Networks, Volume 53, Issue 17, 2009, Pages 2939-2965, ISSN 1389-1286, https://doi.org/10.1016/j.comnet.2009.10.004.

[49] Minde, T.B., Energianvändning i datacenter och digitala system: Rapport till Statens Energimyndighet från RISE i uppdraget "Konsultuppdrag om energianvändningen i datacenter och digitala system", RISE rapport 2023:34, ISBN 978-91-89757-80-6.

[50] Data Centers in Sweden, https://www.datacenters.com/locations/sweden.

[51] Patterson M., et al. ERE: A metric for measuring the benefit of reuse energy from a data center. The Green Grid; 2010.

[52] Oltmanns J. et al., Potential for waste heat utilization of hot-water-cooled data centers: A case study, Energy Sci Eng. 2020;8:1793–1810, DOI: 10.1002/ese3.633.

[53] Dimian A.C. et al., Chapter 20 - Equipment Selection and Design, Computer Aided Chemical Engineering, Elsevier, Volume 35, 2014, Pages 757-788, ISSN 1570-7946, ISBN 9780444627001, https://doi.org/10.1016/B978-0-444-62700-1.00020-6.

[54] RISE data center ICE, https://www.ri.se/en/news/blog/this-is-how-data-centers-work-in-your-everyday-life.

[55] Jeter S.M. et al., Variable speed drive heat pump performance, Energy, Volume 12, Issue 12, 1987, Pages 1289-1298, ISSN 0360-5442, https://doi.org/10.1016/0360-5442(87)90037-5.

[56] Data Centre Review, How To Reduce Energy Consumption in Data Centre, available at: https://datacentrereview.com/2023/05/how-to-reduce-energy-consumption-in-data-centres/ (Accessed 30th May 2023).

[57] Stockholm Exergi, Unleash the market economy for successful heat reuse (Stockholm Exergi), https://celsiuscity.eu/wp-content/uploads/2021/12/StockholmExergi_Open_District_Heating-Celsius_Summit_Webinar_211125.pdf (Accessed 26th May 2023).

[58] M. Wahlroos et al., Future views on waste heat utilization – Case of data centers in Northern Europe, Renewable and Sustainable Energy Reviews 82 (2018) 1749–1764, https://doi.org/10.1016/j.rser.2017.10.058.

[59] ABB Review, How data centers can minimize their energy use, available at: https://new.abb.com/news/detail/66580/how-data-centers-can-minimize-their-energy-use (Accessed 30th May 2023).